Investigations on the Development of Highly Active Titanium Oxide Photocatalysts and their Reactivity for the Oxidation of Organic Compounds

Investigations on the Development of Highly Active Titanium Oxide Photocatalysts and their Reactivity for the Oxidation of Organic Compounds

(高活性な酸化チタン光触媒の開発と有機化合物の酸化反応における反応性に関する研究)

Shirou SAKAI

酒井　史郎

２０１０

Doctoral Thesis at Osaka Prefecture University

Contents

Chapter 1

General Introduction

1. General Introduction

1. Introduction

Environmental pollution on a global scale as well as the lack of natural energy resources have drawn much attention to the vital need for ecologically clean chemical technologies as one of the most urgent challenges facing chemists today. Since the photosensitization effect of a TiO_2 electrode on water electrolysis was first discovered by Honda and Fujishima in 1972 [1], pollution-free photocatalysis by TiO_2 semiconductors has been widely studied in order to achieve the efficient conversion of clean solar energy into useful chemical energy such as hydrogen [2-9]. New systems and processes powered by clean solar energy will not only resolve energy issues caused by the exhaustion of fossil fuels but can also be applied for the abatement of environmental toxins. Along these lines, photocatalysts which can operate under visible and/or solar light irradiation have been strongly desired for applications in the purification and sustenance of our living environment.

Various studies have also been carried out on TiO_2 nano-particles as well as on various Ti-oxide based binary oxides such as TiO_2/SiO_2, TiO_2/Al_2O_3 and TiO_2/B_2O_3 [10-13]. In particular, we have found that the TiO_2 nano-particles of less than 10 nm show a

significant enhancement in photocatalytic reactivity under UV light irradiation. This phenomenon is due to an electronic modification of the TiO_2 nano-sized semiconductors as well as the close existence of the photo-formed electron and hole pairs and their efficient contribution to the photoreactions. These findings have provided new insights into the development of the highly dispersed transition-metal oxide species as single-site catalysts. Moreover, the application of an anchoring method enabled to prepare the molecular or cluster-sized photocatalysts on various supports such as SiO_2, Al_2O_3, various zeolites and mesoporous materials. Highly dispersed Ti-, Cr-, Mo-oxide species incorporated within the cavities or frameworks of zeolites are especially interesting due to their unique local structures such as the four-fold coordinated species and efficient photocatalytic properties for the reduction of CO_2 with H_2O, NO decomposition as well as the selective photoepoxidation of alkene with O_2, as compared with semiconducting photocatalysts [14-24].

Recently, various air-cleaning systems equipped with TiO_2 photocatalysts and UV light sources that reduce volatile organic compounds (VOCs) which cause the so-called “sick house syndrome” are commercially available. However, the removal efficiency of air-cleaning systems still needs to be improved to be as simple and low-cost as possible for widespread applications. Although the deposition of small amounts of Pt particles on the

TiO_2 surface is known to enhance their photocatalytic reactivity [25-29], Pt is too costly for common use in home electrical appliances. Meanwhile, the hybridization of adsorbents such as zeolites or mesoporous materials [14-19, 30-34] with TiO_2 particles has been reported to show elevated photocatalytic reactivity. In the previous report [35], the TiO_2 nano-particles hybridized with siliceous zeolites prepared by an impregnation method as well as a simple mechanical blending method showed higher photocatalytic reactivity for the complete oxidation of gaseous acetaldehyde than TiO_2 catalysts since the siliceous zeolites can efficiently condense acetaldehyde thinly diffused in the gas phase and smoothly supply them onto the TiO_2 photocatalyst surfaces.

The conversion of solar light energy into renewable clean energy is also one of the most challenging research topics in science and technology. The sunlight including near-infrared, visible and ultraviolet light provide tremendous energy of ca. 87 - 308 kJ mol^{-1} so that solar energy should be utilized as efficiently as possible [36-37, 60-64]. It will, thus, be of great importance to develop the effective systems able to convert abundant solar light energy into applicable and sustainable energy resources. At least two systems have been considered for the conversion of sunlight into other renewable energy sources: one is the design of solar cells to convert sunlight into electricity and the other is artificial photosynthesis for the conversion and storage of solar energy into safe

and useful chemical energy such as hydrogen. Although hydrogen is also the focus of much attention as a renewable clean energy alternative, at the moment, we do not have any highly efficient systems to produce hydrogen in an environmentally harmonious way without producing CO_2. From this viewpoint, the photocatalytic or photoelectrochemical decomposition of water to produce hydrogen under solar light irradiation is now of utmost importance.

In this thesis, the development of highly functional Ti-oxide based photocatalysts, i.e., (i) the tetrahedral Ti-oxide species incorporated within the framework of zeolites and mesoporous materials as single-site photocatalysts; (ii) the TiO_2 nano-particles hybridized with hydrophobic zeolite adsorbents in practical applications for photocatalytic air-cleaning systems; and (iii) the TiO_2 thin films to photocatalytically decompose H_2O into H_2 and O_2 under solar light irradiation will be discussed.

Chapter2

The synthesis, characterization and photocatalytic performance of the TiO_2 nanopowders prepared by a flame-synthesis method were investigated. The photo-excited states of TiO_2 nanopowders under UV-light irradiation were directly observed by an in-situ NEXAFS (Near Edge X-ray Absorption Fine Structure) study. It was found that the anatase/rutile phase boundary works as an electron trapping site. By the combination of

TEM images, the enhancement of the photoreactivity of the TiO_2 nanopowders was attributed to both the changes in the particle shape and the existence of an anatase/rutile phase boundary, on which the excited electrons have long lifetimes and suppress the recombination of the photo-formed electrons and holes.

Chapter3

TiO_2 photocatalysts were prepared by a multi-gelation method and the effect of the changes in the pH of the pH swing method, on the morphology of the TiO_2 particles was investigated. The photocatalytic properties of the TiO_2 nano-powder prepared by the controlled pH swing method were compared with the TiO_2 particles prepared without adjusting the pH value during the swing times. The photocatalytic performances of these TiO_2 nano-powders were investigated by comparing the photocataliyic degradation reaction of 2-propanol under UV light irradation. The experimental results showed that the TiO_2 photocatalysts prepared without adjusting the pH showed better performance in controlling the important parameters of the catalysts such as the particle size, surface area, anatase/rutile phase ratio, the pore size as well as pore volume than the TiO_2 photocatalysts prepared by a controlled pH swing method.

Chapter4

The photocatalytic oxidation of gaseous acetaldehyde with O_2 on the commercial TiO_2 nano-particles could be successfully enhanced by a simple mechanical blending with a

siliceous mordenite (MOR) zeolite, which showed highly hydrophobic surface. When the TiO_2 nano-particles of ca. 5 - 20 wt% were mixed with the MOR zeolite powders in an agate mortar for only 5 min, the blended TiO_2/MOR samples showed higher photocatalytic reactivity as compared with the pure untreated TiO_2 nano-particles. Since the siliceous zeolite powders are highly transparent in UV-VIS light regions, the incident UV light is effectively irradiated onto the whole part of the TiO_2 nano-particles without any loss of light intensity. Furthermore, the hydrophobic MOR zeolite powders effectively adsorb the gaseous acetaldehyde molecules and supply them onto the surfaces of the blended TiO_2 nano-particles, resulting in the enhancement of the photocatalytic reactivity.

Chapter5

TiO_2 thin film photocatalysts which could induce photoreactions under visible light irradiation were successfully developed in a single process by applying an ion engineering technique, i.e., a RF magnetron sputtering deposition method. The TiO_2 thin films prepared at higher than 773 K showed the efficient absorption of visible light, on the other hand, the TiO_2 thin films prepared at around 473 K was highly transparent. This clearly means that the optical properties of the TiO_2 thin films, which absorb not only UV but also visible light, can be controlled by the preparation temperatures of the RF magnetron

sputtering deposition method. These visible light responsive TiO_2 thin films were found to exhibit effective photocatalytic reactivity under visible light irradiation ($\lambda > 450$ nm) at 275 K for the reductive decomposition of NO into N_2 and N_2O. From various characterizations, the orderly aligned columnar TiO_2 crystals could be observed only for the visible light responsive TiO_2 thin films. This unique structural factor is expected to modify the electronic properties of TiO_2 semiconductor, enabling the efficient absorption of visible light.

Chapter6

These conclusions obtained from the investigations covered in this thesis have been summarized in this chapter.

References

[1] K. Honda, A. Fujishima, Nature 238 (1972) 37.

[2] T. Inoue, A. Fujishima, S. Konishi, K. Honda, Nature 277 (1979) 637.

[3] T. Kawai, T. Sakata, Nature 286 (1980) 31.

[4] G. N. Schrauzer, A. J. Bard, J. Am. Chem. Soc. 99 (1977) 7189.

[5] A. Heller, A. A. Shalom, W. A. Bonner, B. Miller, J. Am. Chem. Soc. 104 (1982) 1688.

[6] M. A. Fox, Acc. Chem. Res. 16 (1983) 314.

[7] S. Sato, J. M. White, J. Am. Chem. Soc. 102 (1980) 7206.

[8] H. Courbon, J. M. Herrmann, P. Pichat, J. Catal. 72 (1981) 129.

[9] M. Anpo, in: G. Ertl, H. Knözinger, J. Weitkamp (Eds.), Handbook of Heterogeneous Catalysis, Wiley-VCH, Weinheim, 1997, and references therein.

[10] M. Anpo, T. Shima, Y. Kubokawa, Chem. Lett. (1985) 1799.

[11] M. Anpo, H. Nakaya, S. Kodama, Y. Kubokawa, K. Domen, T. Onishi, J. Phys. Chem. 90 (1988) 1633.

[12] M. Anpo, T. Kawamura, S. Kodama, K. Maruya, T. Onishi, J. Phys. Chem. 92 (1988) 438.

[13] H. Yamashita, S. Kawasaki, Y. Ichihashi, M. Harada, M. Takeuchi, M. Anpo, J.

Phys. Chem. B 102 (1998) 5870.

[14] M. Anpo, H. Yamashita, K. Ikeue, Y. Fujii, S.G. Zhang, Y. Ichihashi, D.R. Park, Y. Suzuki, K. Koyano, T. Tatsumi, Catal. Today 44 (1998) 327.

[15] H. Yamashita, Y. Fujii, Y. Ichihashi, S.G. Zhang, K. Ikeue, D.R. Park, K. Koyano, T. Tatsumi, M. Anpo, Catal. Today 45 (1998) 221.

[16] S.G. Zhang, Y. Fujii, H. Yamashita, K. Koyano, T. Tatsumi, M. Anpo, Chem. Lett. (1997) 659.

[17] M. Anpo, H. Yamashita,Y. Ichihashi, Y. Fujii, M. Honda, J. Phys. Chem. B, 101 (1997) 2632.

[18] M. Matsuoka, M. Anpo, J. Photochem. Photobiol. C: Photochem. Rev. 3, (2003) 225.

[19] M. Anpo (Ed.), Photofunctional Zeolites, NOVA, 2000.

[20] A. Corma, Chem. Rev. 97 (1997) 2373.

[21] T. Maschmeyer, F. Rey, G. Sankar, J. M. Thomas, Nature 378 (1995) 159.

[22] L. Marchese, T. Maschmeyer, E. Gianotti, S. Coluccia, J. M. Thomas, J. Phys. Chem. B 101 (1997) 8836.

[23] C. Lamberti, S. Bordiga, D. Arduino, A. Zecchina, F. Geobaldo, G. Spano, F. Genoni, G. Petrini, A. Carati, F. Villain, G. Vlaic, J. Phys. Chem. B 102 (1998)

6382.

[24] H. Yamashita, K. Yoshizawa, M. Ariyuki, S. Higashimoto, M. Che, M. Anpo, J. Chem. Soc. Chem. Commun. (2001) 435.

[25] S. Sato and J. M. White, Chem. Phys. Lett. 72 (1980) 83.

[26] M. Grätzel (Ed.), "Energy Resources through Photochemistry and Catalysis" Academic Press, New York (1983).

[27] M. Anpo, T. Shima, S. Kodama, Y. Kubokawa, J. Phys. Chem. 91 (1987) 4305.

[28] M. Anpo, K. Chiba, M. Tomonari, S. Coluccia, M. Che, M. A. Fax, Bull. Chem. Soc. Jpn. 64, 543 (1991).

[29] M. Takeuchi, K. Tsujimaru, K. Sakamoto, M. Matsuoka, H. Yamashita, M. Anpo, Res. Chem. Intermed., 29, 6, 619 (2003).

[30] N. Takeda, T. Torimoto, S. Sampath, S. Kuwabata, H. Yoneyama, J. Phys. Chem. 99 (1995) 9986.

[31] V. Durgakumari, M. Subrahmanyam, K.V. Subba Rao, A. Ratnamala, M. Noorjahan, K. Tanaka, Appl. Catal. A Gen. 234 (2002) 155.

[32] M. Anpo, M. Che, Adv. Catal., 44 (2000) 119.

[33] K.D.M. Harris, P. Edwards (Eds.), "Turning Points in Solid-State, Materials and Surface Science", RSC Publishing, Cambridge (2008).

[34] H. Yamashita, S. Kawasaki, S. Yuan, K. Maekawa, M. Anpo, M. Matsumura, Catal. Today, 126 (2007) 375.

[35] M. Takeuchi, T. Kimura, M. Hidaka, D. Rakhmawaty, M. Anpo, J. Catal., 246 (2007) 235.

[36] M. Matsuoka, M. Kitano, M. Takeuchi, M. Anpo, J. M. Thomas, Topics Catal., 35 (2005) 305.

[37] M. Kitano, K. Tsujimaru, M. Anpo, Topics Catal., 49 (2008) 4.

[38] H. Yamashita, M. Anpo, Surf. Sci. Jpn. 17 (1996) 30.

[39] S. G. Zhang, Y. Ichihashi, H. Yamashita, T. Tatsumi, M. Anpo, Chem. Lett. (1996) 895.

[40] M. Anpo, S. G. Zhang, S. Higashimoto, M. Matsuoka, H. Yamashita, Y. Ichihashi, Y. Matsumura, Y. Souma, J. Phys. Chem. B 103 (1999) 9295.

[41] J. Zhang, M. Minagawa, M. Matsuoka, H. Yamashita, M. Anpo, Catal. Lett. 66 (2000) 241.

[42] J. Zhang, M. Matsuoka, H. Yamashita, M. Anpo, J. Synchrotron Radiat. 8 (2001) 637.

[43] J. Zhang, M. Minagawa, T. Ayusawa, S. Natarajan, H. Yamashita, M. Matsuoka, M. Anpo, J. Phys. Chem. B 104 (2000) 11501.

[44] M. Anpo, M. Kondo, S. Coluccia, C. Louis, M. Che, J. Am. Chem. Soc. 111 (1989) 8791.

[45] S. G. Zhang, M. Ariyuki, H. Mishima, S. Higashimoto, H. Yamashita, M. Anpo, Micropor. Mesopor. Mater. 21 (1998) 621.

[46] S. G. Zhang, S. Higashimoto, H. Yamashita, M. Anpo, J. Phys. Chem. B 102 (1998) 5590.

[47] K. Ikeue, H. Yamashita, M. Anpo, Chem. Lett. (1999) 1135.

[48] K. Ikeue, H. Yamashita, M. Anpo, J. Phys. Chem. B 105 (2001) 8350.

[49] K. Ikeue, S. Nozaki, M. Ogawa, M. Anpo, Catal. Lett. 80 (2002) 111.

[50] D. R. Park, J. Zhang, K. Ikeue, H. Yamashita, M. Anpo, J. Catal. 185 (1999) 114.

[51] M. Ogawa, K. Ikeue, M. Anpo, Chem. Mater. 13 (2001) 2900.

[52] K. Ikeue, H. Yamashita, M. Anpo, T. Takewaki, J. Phys. Chem. B 105 (2001) 8350.

[53] M. Takeuchi, J. Deguchi, M. Hidaka, S. Sakai, K. Woo, P. Choi, J. Park, M. Anpo, Appl. Catal. B: Environ., (in print) (2009).

[54] Y. Paz, Z. Luo, L. Rabenberg, A. Heller, J. Mater. Res., 10, 11, (1995) 2842.

[55] A. Heller, Acc. Chem. Res., 28, (1995) 503.

[56] N. Negishi, T. Iyoda, K. Hashimoto and A. Fujishima, Chem. Lett., (1995) 841.

[57] N. Negishi, K. Takeuchi and T. Ibusuki, J. Mater. Sci., 33, (1998) 1.

[58] M. Takeuchi, H. Yamashita, M. Matsuoka, T. Hirao, N. Itoh, N. Iwamoto and M. Anpo, Catal. Lett., 67, (2000) 135.

[59] M. Takeuchi, H. Yamashita, M. Matsuoka, T. Hirao, N. Itoh, N. Iwamoto and M. Anpo, Catal. Lett., 66, (2000) 185.

[60] M. Kitano, M. Tsujimaru, M. Anpo, Appl. Catal. A: Gen., 314 (2006) 179.

[61] H. Kikuchi, M. Kitano, M. Takeuchi, M. Matsuoka, M. Anpo, P.V. Kamat, J. Phys. Chem. B, 110 (2006) 5537.

[62] M. Kitano, K. Funatsu, M. Matsuoka, M. Ueshima, M. Anpo, J. Phys. Chem. B, 110 (2006) 25266.

[63] M. Matsuoka, M. Kitano, M. Takeuchi, K. Tsujimaru, M. Anpo, J.M. Thomas, Catal. Today, 122 (2007) 51.

[64] M. Kitano, M. Takeuchi, M. Matsuoka, J.M. Thomas, M. Anpo, Cat. Today, 120 (2007) 133.

[65] S. A. Bilmes, P. Mandelbaum, F. Alvarez, and N. M. Victoria, J. Phys. Chem. B, 104, (2000) 9851.

Chapter 2

Suppressed Recombination of Electrons And Holes And its role in the improvement of the Photoreactivity of Flame-synthesized TiO_2 Nanopowders

2. Suppressed Recombination of Electrons and Holes and its role in the improvement of the Photoreactivity of Flame-synthesized TiO_2 Nanopowders

2.1. Introduction

Titanium dioxide (TiO_2) is well-known as an effective photo-functional material which exhibits photocatalytic properties for ractions in environmental purification, hydrogen production from water, and superheydrophilic properties under UV-light irradiation. Many researchers have, thus far, endeavoured to improve its photocatalytic efficiency by different synthetic techniques. TiO_2 photocatalysts have been fabricated using such methods as sol-gel, hydrothermal treatment, and other physical methods [1-3]. Among them, the flame synthesis approach is one of the most effective in preparing TiO_2 nanopowders with high photocatalytic performance [4-6]. In general, the flame synthesis of TiO_2 nanopowders is carried out at high temperatures above 900℃, affording TiO_2 nanoparticles with very high degrees of crystallinity. Therefore, no additional calcination at high temperature is necessary to improve the crystallinity [7-12]. This fabrication method results in a low degree of agglomeration of the TiO_2 nanoparticles, which is crucial to obtaining high dispersibility in liquid media as well as a large specific surface

area. Moreover, the properties of a synthesized TiO_2 nanopowder can be modified by post-treatments such as surface etching in acid solution [13] and heat-treatment at elevated temperatures in a controlled atmosphere [4, 14]. However, such post-treatments of a TiO_2 nanopowder are not always effective since the physico-chemical properties of TiO_2 nanopowders such as the lattice defects inside the bulk and anatase-to-rutile phase ratios are often controlled by the synthesis method.

Along these lines, we report on the effect of heat-treatment of TiO_2 nanopowders prepared by the flame-synthesis method. In particular, attention is focused on the relationship between the photo-excited structure and the photocatalytic performance of the TiO_2 nanopowders.

2.2. Experimental

2.2.1. Preparation of the Photocatalysts

The TiO_2 nanopowders were synthesized by a flame synthesis method using titanium tetra-isopropoxide (TTIP, Aldrich, 97 %) as a precursor. The TTIP was vaporized in an oil bath and delivered to the burner nozzle along with nitrogen gas as a carrier gas. The TTIP vapor was mixed with oxygen gas (an oxidizer) and methane gas (a fuel) in a burner and

combusted. The resultant TiO_2 nanoparticles loaded in the flowing product gas were transported to the collection chamber and separated from the product gas by filtration through a High Airflow Particulate Air (HAPA) filter. The obtained TiO_2 nanopowder (hereafter referred to as the as-synthesized TiO_2 nanopowder) was heat treated at 400, 500, 600, 700, 800 or 900℃ for 1 h in air. Hereafter, the heat-treated powders are referred to as HTxxx, where xxx indicates the treatment temperature in Celsius degrees.

2.2.2. Characteriztaion of crystalline and electronic structures

The as-synthesized and heat-treated TiO_2 nanopowders were characterized using X-ray diffraction to identify the constituent phase(s) and particle size (XRD; Bruker D8 Advance), [17] and transmission electron microscopy to determine the shape and size of the particles (TEM; FEI Technai G^2.)

The photo-excited structures of the TiO_2 nanopowders under UV light irradiation were directly observed by NEXAFS (Near-Edge X-ray Absorption Fine Structure; 7B1 KIST B/L at the Pohang Accelerating Laboratory (PAL), Korea). The powder samples were compacted into thin disks without using any polymer binder in order to prevent surface changes and additional effects associated with polymer binders. Two kinds of 8W UV-lamps, radiating UVA (λ= 320 - 400 nm) and UVB (λ= 280 - 320 nm), were installed

together in the NEXAFS chamber. The compacted disk was mounted on the specimen holder and positioned vertically beneath the UV lamp. The UV lamp was located at a distance of 50 cm from the disc, forming an angle of 15 degrees from the normal line. Prior to data acquisition, the NEXAFS chamber was evacuated to 10^{-9} Torr. The incident beam was irradiated perpendicular to the substrate surface and the resultant photo-currents were recorded. The oxygen K-edge spectra were recorded for every sample under the same normal NEXAFS conditions prior to turning on the UV lamp. Additional oxygen K-edge spectra were obtained twice for every sample under sequential irradiation with UVA followed by UVB and these NEXAFS spectra are referred to as UVA and UVB. Just after turning off the UVB lamp, two additional scans of the compacted disk (called OFF1 and OFF2) were performed.

2.2.3. Photoctalytic performance

The photoreactivity of the TiO_2 nanopowders was analyzed for the photo-degradation of 2-propanol into CO_2 on the TiO_2 photocatalysts under UV light irradiation. An amount of 50 mg of the TiO_2 nanopowder was suspended in a quartz cell containing an aqueous solution of 2-propanol (2.6×10^{-3} mol·dm^{-3}, 25 mL). Prior to UV light irradiation, the suspension was stirred for 30 min under oxygen atmosphere in the dark. The suspension

was then continuously stirred under oxygen atmosphere at 295 K and simultaneously irradiated with UV light (λ> 254 nm) emitted from a 100 W high-pressure Hg lamp. An amount of 2 mL of the suspension was taken at regular intervals, filtered through a Millipore filter to separate the TiO_2 particles from the solution, and then analyzed by gas chromatography.

2.3 Results and discussion

2.3.1. Characterization of the TiO_2 photocatalysts

The morphology of the TiO_2 was investigated by TEM spectroscopy and TEM images of the as-synthesized and heat-treated TiO_2 nanopowders are shown in Fig. 2.1. The shape of the as-synthesized TiO_2 nanopowder is spherical, while that of HT500 changes to euhedral (Fig. 2.1b), while that of HT600, HT700, HT800 and HT900 change to an octagonal structure and/or cuboidal, as shown in Fig. 2.1c-f. The inset of each image shows the detailed morphologies of the TiO_2 particles in high magnification. It is clearly shown that inter-particle boundaries are evident on the TiO_2 after heat treatment above 700℃. Thus, heat treatment of the TiO_2 nanopowders was observed to lead to changes in the morphology below 700℃, probably due to the surface relaxation enhanced by surface

diffusion with the assisted mobility of the atoms.

Figure 2.2 shows the XRD patterns of the TiO_2 nanopowders as a function of the heat treatment temperatures. It is observed that the XRD patterns apparently change from an anatase to rutile phase at a heat treatment temperature of 800℃. The particle size of the anatase and rutile phase of TiO_2, which was calculated by the Scherer equation and the content of the rutile phase in each TiO_2 nanopowder are shown in Fig. 2.3. The as-synthesized TiO_2 involves ca. 98 % anatase phase together with ca. 2 % rutile phase. The transition state from anatase to rutile takes place at above 700℃ and is completed at 900℃. The ratio of the rutile/anatase phase change was ca. 5 % at 700℃, ca. 23 % at 800℃, and ca. 99 % at 900℃. On the other hand, the particle size of the anatase phase slightly increases from 50 nm to 55 nm by heat treatment up to 800℃, while that of the rutile phase is estimated at ca. 67.5 nm at 900℃.

In order to identify the presence of the anatase-rutile phase boundary in the HT800 powder, several dumbbell-type particles were closely observed by TEM analysis. Figure 2.4 shows the image of the HT800 powder dispersed in ethanol with ultrasonic treatment. A grain boundary composed of the anatase-rutile phase on the HT800 which chemically interact with each other is clearly observed.

2.3.2. Evaluation of the photocatalytic activity

Figure 2.5 shows the photocatalytic reactivity for the degradation of 2-propanol on the as-synthesized and heat-treated TiO_2 nanopowders. It is observed that the degradation of 2-propanol takes place in proportion to the irradiation time on the TiO_2 photocatalysts under UV-light irradiation. The degradation rate of 2-propanol increases with an increase in the heat-treatment temperature up to 800℃, as shown in Fig. 2.5. Furthermore, the degradation rate of 2-propanol drastically decreased on HT900 due to the rutile phase, showing poor photocatalytic activity [17].

2.3.3. Photo-excited state of TiO_2 under UV-light irradiation

NEXAFS was applied to investigate the photo-excited structure of TiO_2. The electronic structures are affected in its photo-excitation energy by the wavelength of the incident light and such influences are assumed to change the NEXAFS spectra [18-20]. Figure 2.6 shows the NEXAFS spectra of the oxygen K-edge of the TiO_2 nanopowders. As can be seen, peaks at ca. 531-533 eV and 529-530.5 eV can be observed and they are attributed to the transitional absorption of the t_{2g} and e_g states of oxygen on TiO_2 having an anatase structure, respectively. In the present study, we determined the variations in the relative peak intensity between the t_{2g} and e_g levels as well as the peak position as a function of the

heat-treatment temperature. It should be noted that spectral quality during photo-irradiation showed serrated curves, irrespective of the samples. The as-synthesized TiO_2 nanopowder shows almost no change in the relative peak intensity of t_{2g} and e_g under different conditions (Fig. 2.6a). On the other hand, it was observed that UV-light irradiation of T600, T700 and T800 induces an increase in the peak of t_{2g}, whose height is close to that of e_g. Subsequently, T700 and T800 retained relative peak intensity at Stage OFF1 (over 30 min.). These results suggest that the recombination of the electrons with holes in the valance band is significantly suppressed, as shown in Fig 2.7. Furthermore, the phenomenon observed in HT900 is similar to that of the as-synthesized TiO_2 sample (data not shown).

2.3.4. Relationship between photo-excited structures of TiO_2 and their photocatalytic performance

The rate of photocatalytic degradation increases in temperatures up to 700℃ despite no significant differences in phase transition among HT500, HT600 and HT700, as shown in Fig. 2.2. From the TEM images, it is observed that an improvement in the photocatalytic degradation on the TiO_2 heat-treated up to 700℃ is due to the changes in the particle shape of the TiO_2. Further improvement in the photocatalytic properties of HT800 is

attributed to the presence of the anatase/rutile phase boundary [15-16], as shown in Figs. 2.2 and 2.3, since the boundary between the anatase and rutile phases at 800℃ causes effective trapping of the photo-induced electrons, with a long lifetime in their excited states. On the other hand, drastic deactivation on HT900 is attributed to the dominant rutile phase.

2.4. Conclusions

Anatase phase-rich TiO_2 nanopowders containing small amounts of the rutile phase were fabricated by the flame method. The photoexcited states of the TiO_2 nanopowders were directly determined by in-situ NEXAFS measurements under UV light irradiation. The present findings provide unprecedented direct experimental evidence by in-situ NEXAFS analysis showing that the electrons trapped in the anatase/rutile grain boundary suppress the recombination of electrons and holes, and in turn, this suppression of recombination directly contributes to an improvement in the photocatalytic reactivity for the decomposition of 2-propanol.

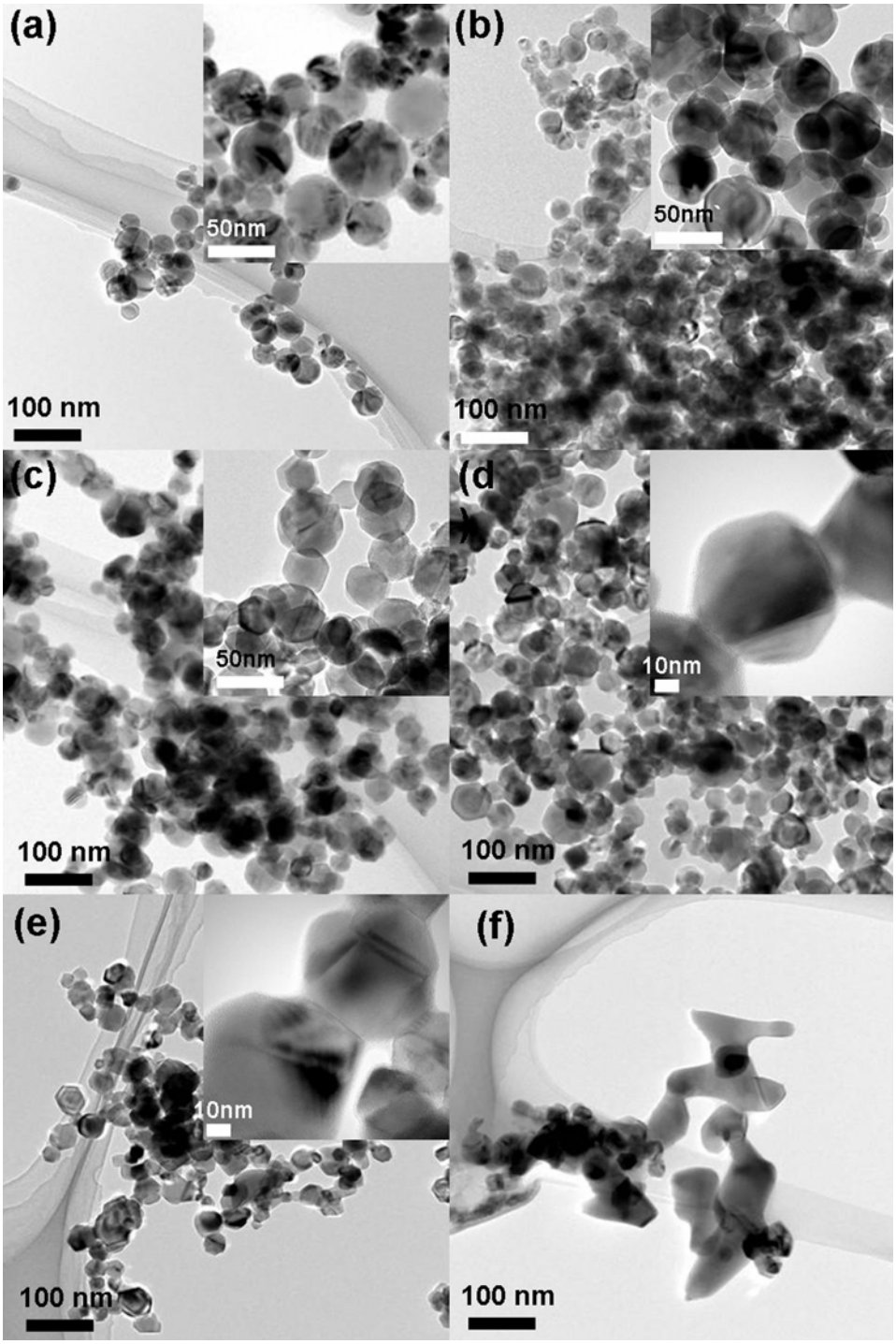

Figure 2.1. TEM images of TiO_2 nanopowders: (a) as-synthesized, (b) HT500, (c) HT600, (d) HT700, (e) HT800, (f) HT900.

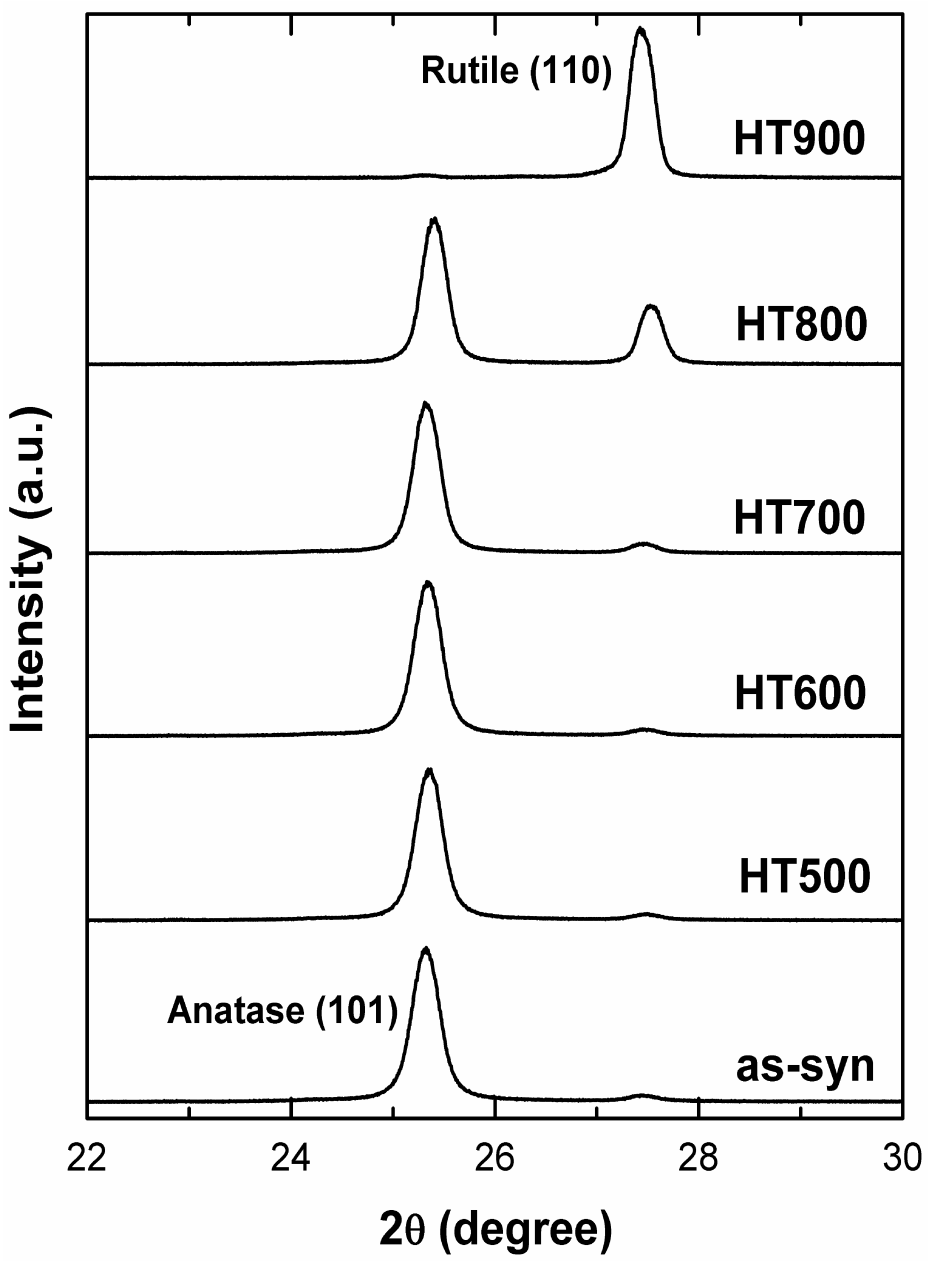

Figure 2.2. XRD patterns of the as-synthesized and annealed TiO_2 nanopowders.

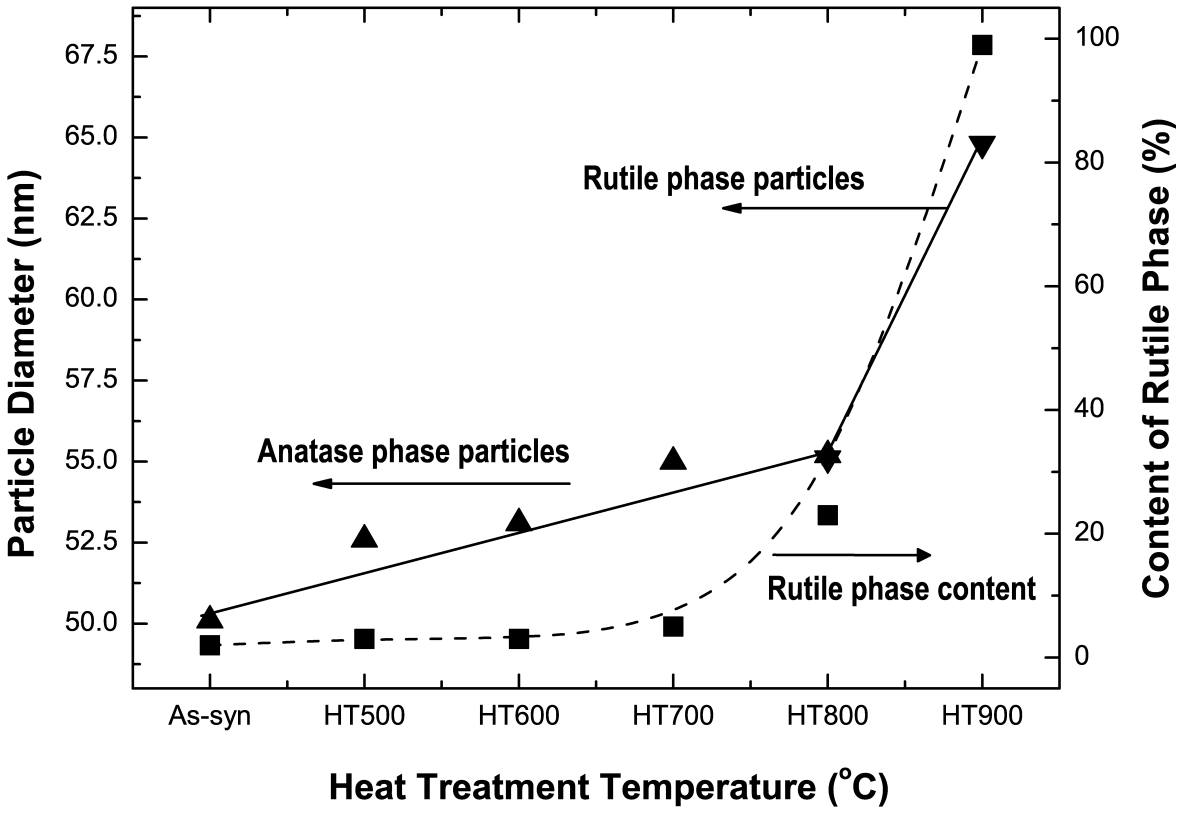

Figure 2.3. Variations in TiO_2 particle size and content in the rutile phase for powders with heat treatment.

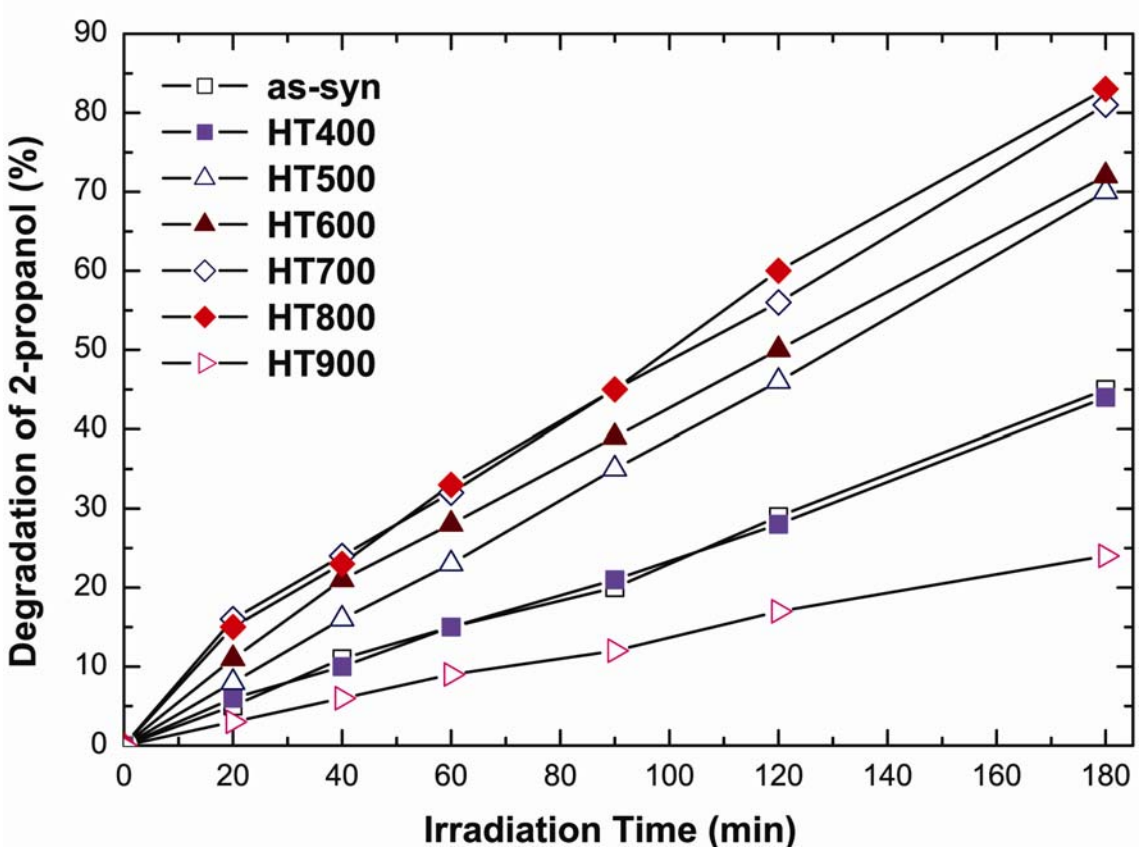

Figure 2.4. Photocatalytic degradation of 2-propanol under UV irradiation by various kinds of TiO_2 nanopowders (as-synthesized and heat treated).

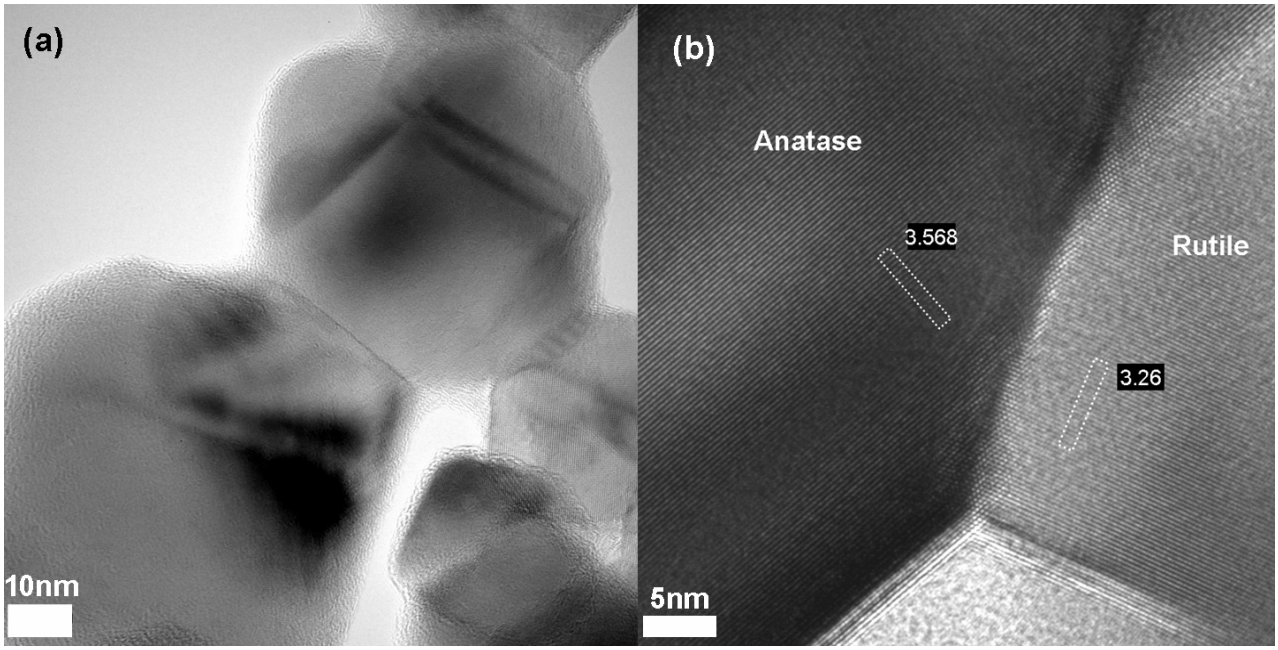

Figure 2.5. TEM images showing the anatase-rutile phase boundary in the TiO_2 nanopowder treated at 800℃: (a) Low magnification, and (b) High magnification images.

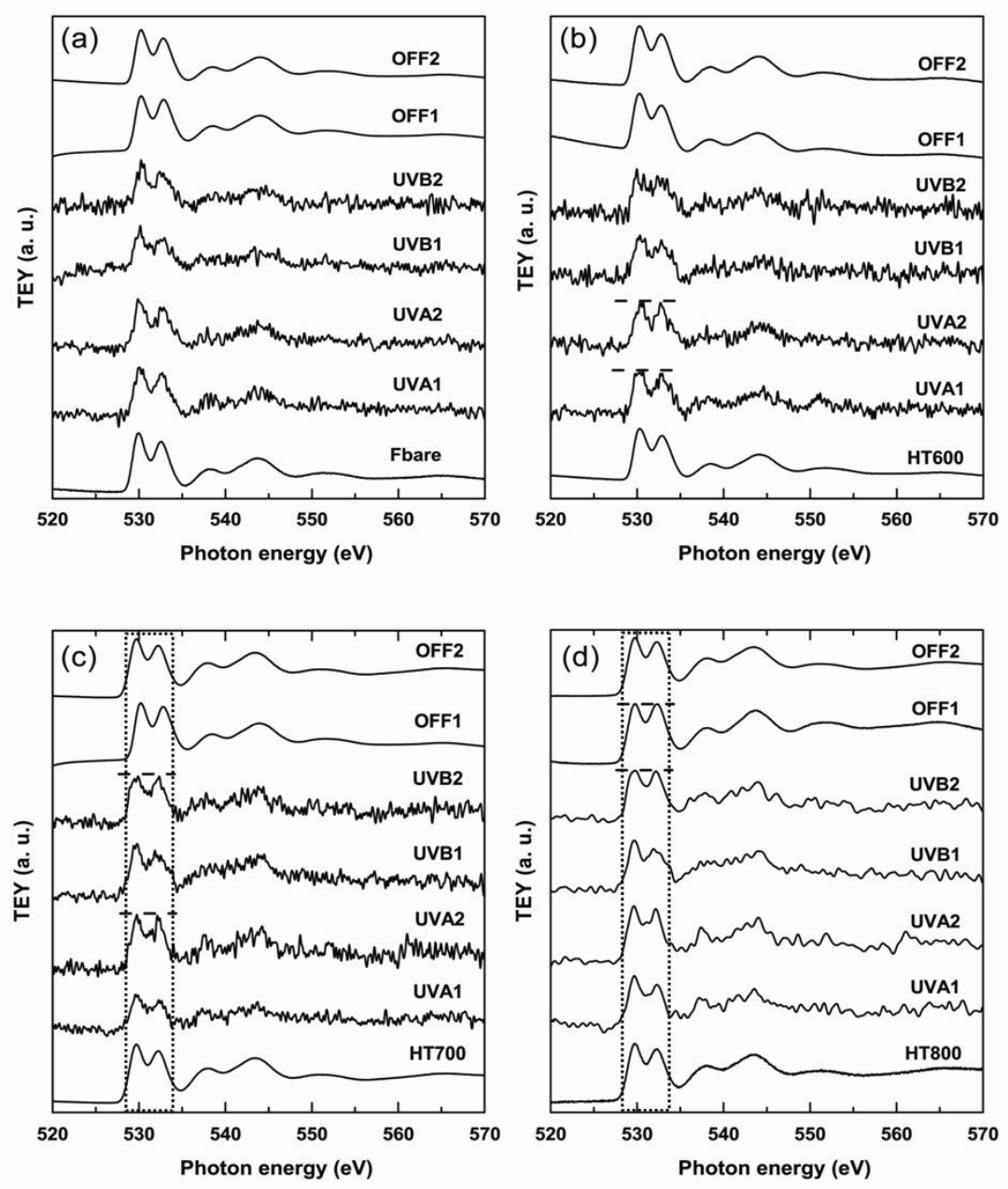

Figure 2.6. Variations in oxygen K-edge spectra of TiO_2 nanopowders under UV irradiation: (a) as-synthesized, (b) HT600, (c) HT700, (d) HT800.

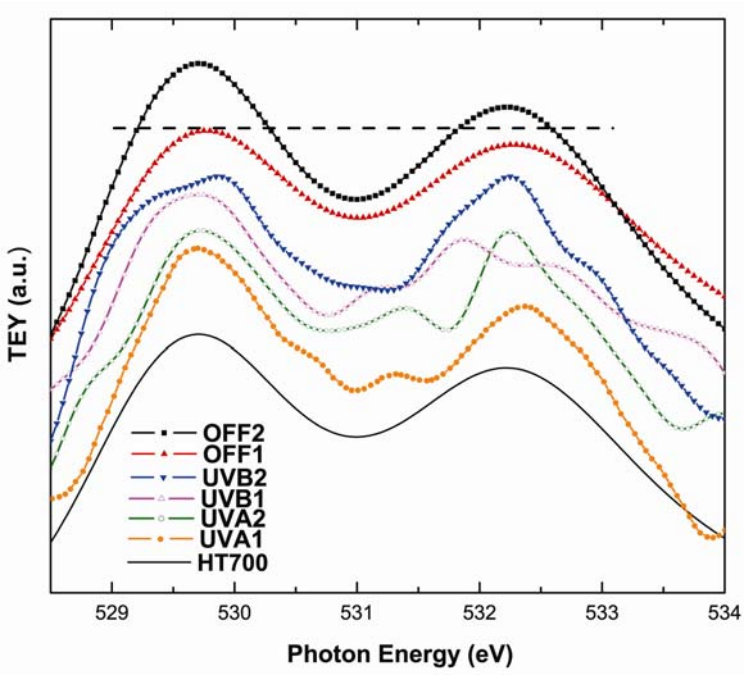

(a)

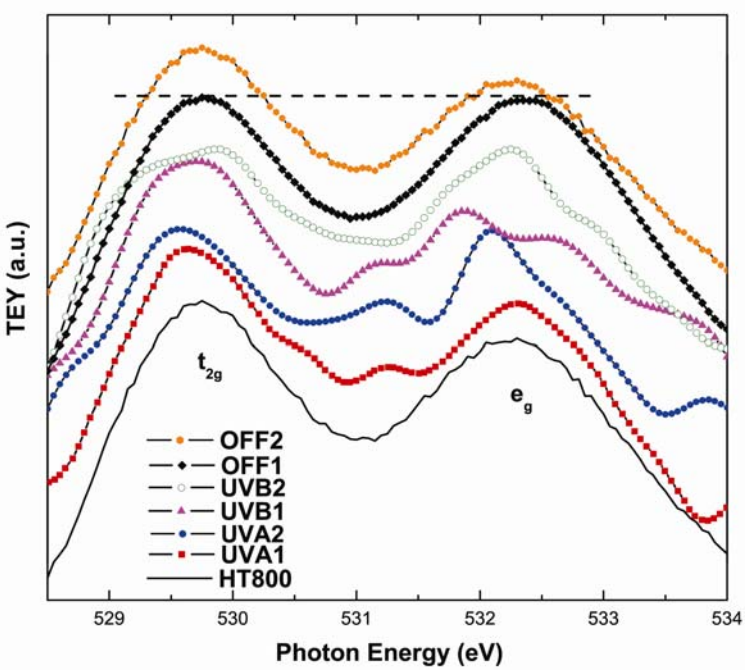

(b)

Figure 2.7. NEXAFS O K-edge spectra of: (a) HT700, (b) HT800 (part of Figs. 6(c) and (d))

2.5. References

[1] C. H. Cho, M.H. Han, D.H. Kim and D.K. Kim, Mater. Chem. Phys. 92 (2005) 104.

[2] T. Ohno, K. Sarukawa and M. Matsumura, J. Phys. Chem. B 105 (2001) 2417.

[3] K. Nakaso, K. Okuyama, M. Shimada and S. Pratsinis, Chem. Eng. Sci. 58 (2003) 3327.

[4] S. U. Khan, M. U. M. Al-Shahry and W. B. Ingler Jr, Science 297 (2002) 2243.

[5] B. Neppolian, H. S. Jie, J. P. Ahn, J. K. Park and M. Anpo, Chem. Lett. 33 (2004) 1562.

[6] H. Park, B. Neppolian, H. S. Jie, J.P. Ahn, J. K. Park, M. Anpo and D. Y. Lee, Curr. Appl. Phys 7 (2007) 118.

[7] C. B. Almquist and P. Biswas, J. Catal. 212 (2002) 145.

[8] J-H. Lee and Y-S. Yang, Mater. Chem. Phys. 93 (2005) 237.

[9] H. Wang, Y. Wu and B-Q. Xu, Appl. Catal. B: Environ. 59 (2005) 139.

[10] C.K. Chan, J.F. Porter, Y-G. Li, W. Guo and C-H, Chan, J. Am. Ceram. Soc. 82 (1999) 566.

[11] C.H. Cho, D.K. Kim and D.H. Kim, J. Am. Ceram. Soc. 86 (2003) 1138.

[12] J.F. Porter, Y. Li and C.K. Chan, J. Mater. Sci. 34 (1999) 1523.

[13] T. Taguchi, Y. Saito, K. Sarukawa, T. Ohno and M. Matsumura, New. J. Chem. 27

(2003) 1304.

[14] S. Yang and L. Gao, J. Am. Ceram. Soc. 88 (2005) 968.

[15] T. Miyagi, M. Kamei, T. Mitsuhashi, T. Ishigaki, and A. Yamazaki, Chem. Phys. Lett. 390 (2004) 399.

[16] D. C. Hurum, A. G. Agrios, K. A. Gray, T. Rajh and C. Thurnauer, J. Phys. Chem. B 107 (2003) 4545.

[17] Yu. V. Kolen, B. R. Churagulv, M. Kunst, L. Mazerolles and C. Colbeau-Justin, Appl. Catal. B : Environ. 52 (2004) 51.

[18] J. G. Chen, Surf. Sci. Rep. 30 (1997) 1.

[19] G. S. Herman, Z. Dohnalek, N. Ruzycki and U. Diebold, J. Phys. Chem. B 107 (2003) 2788.

[20] Bo Sun and Panagiotis G. Smirniotis, Catal. Today 88 (2003) 49.

Chapter 3

Preparation of TiO_2 nano-particle photocatalysts by a multi-gelation method: The effect of pH change

3. Preparation of TiO_2 nano-particle photocatalysts by a multi-gelation method: The effect of pH change

3.1. Introduction

TiO_2 catalysts can be applied for various purposes, e.g., as photocatalysts for pollution abatement [1-3], use in pigments [4], water splitting reactions [5], and solar cells [6], etc. They have been used extensively in environmental remediation processes due to their potential in oxidizing toxic organic compounds into CO_2 and water. However, continuous efforts to improve their reactivity are essential in order to realize their large scale global application and, presently, various methods are being investigated for the development of such highly efficient photocatalysts. Thus far, various preparation methods in which the photocatalytic activity of the TiO_2 particles depend on the preparation conditions have been reported [7-16]. In line with such work, we have prepared TiO_2 photocatalysts by employing various approaches such as the pH swing method [5, 11-16]. The pH swing method enables control of the intrinsic as well as extrinsic properties of the TiO_2 photocatalysts by a simple change in the pH of the reaction mixture during preparation [14]. An earlier pH swing method followed the principle of alternating the addition of $TiCl_4$ (as an acid solution) and aqueous ammonia (as a basic solution) to water at regular

intervals without adjusting the pH of the reaction mixture [14]. In the present study, the pH of the solution was kept constant at around 2 using HCl acid and at 8 using aqueous ammonia during preparation. The effect of the change in pH by a controlled pH swing method on the morphology of the TiO_2 particles as well as its application in the photocatalytic degradation ability of 2-propanol were investigated and compared with the photocatalytic properties of TiO_2 catalysts prepared by an uncontrolled pH swing method.

3.2. Experimental

Catalyst preparation

A $TiCl_4$ solution was prepared by mixing equal weights of $TiCl_4$ (obtained from Wako Chemicals, Japan) with crushed ice made from distilled water. TiO_2 catalysts were prepared by continuous heating and stirring of the $TiCl_4$ solution (500 mL) with an aqueous ammonia solution (14 wt%, 710 mL) under different pH swings at 353 K. A white precipitate of TiO_2 was prepared, filtered and dried at 393 K for 15 hrs. The dried TiO_2 was calcined at various temperatures with an electric furnace under a flow of air. Similarly, TiO_2 photocatalysts were prepared by a controlled pH swing method. In this method, 1 M HCl acid was used to bring down the pH to around 2 at each swing time and aqueous ammonia was used to adjust the pH to around 8.

Catalyst characterizations

The diffuse reflectance absorption spectra of the photocatalysts were recorded with a Shimadzu UV-2200A spectrophotometer at 297 K. X-ray diffraction patterns of the photocatalysts were obtained with a Rigaku RDA- ٧A X-ray diffractometer using Cu Kα radiation with a Nickel filter. The N_2 BET surface area of the TiO_2 catalysts was also determined. The pore volume and pore diameter were determined by a BET analyzer (Micromeritics, ASAP 2020, USA)..

Photocatalytic activity measurements

The photocatalytic activity was investigated by comparing the reaction rates for the oxidative degradation of 2-propanol in which 2-propanol was seen to be completely oxidized into CO_2 and water on the TiO_2 photocatalysts under UV light irradiation in the presence of water and oxygen. The photocatalyst (50 mg) was suspended in a quartz cell with an aqueous solution of 2-propanol (2.6×10^{-3} mol dm^{-3}, 25 mL). Prior to UV light irradiation, the suspension was stirred for 30 min under oxygen atmosphere in dark conditions. The sample was then irradiated at 297 K using UV light ($\lambda > 250$ nm) from a 100 W high-pressure Hg lamp with continuous stirring under oxygen atmosphere in the

system. At periodic intervals, 2 mL aliquots were taken from the system, centrifuged, and then filtered through a Millipore filter to remove the TiO_2 particles. The products were then analyzed by gas chromatography.

3.3. Results and discussion

The XRD patterns of the TiO_2 photocatalysts showed the existence of well crystalline particles prepared by both uncontrolled pH swing (hereafter denoted as the flexible pH method) and controlled pH swing (hereafter denoted as the fixed pH method) and calcined above 450 °C (Fig. not shown). Figure 3.1 shows the anatase phase content of the TiO_2 particles prepared by both methods and calcined at 650°C. The catalysts calcined at 650°C under both preparation methods were comparable in terms of their catalytic properties. Thus, samples calcined at 650°C were used as the representative catalysts for a comparative study of both methods. Figure 3.1 clearly shows that the photocatalysts prepared by the fixed pH method (pH Fix) is able to prevent a phase transition, i.e., from anatase to rutile, irrespective of an increase in the number of pH swings and with calcination treatment at 650°C, whereas, in the flexible pH method (pH Fle), the anatase phase gradually increased with an increase in the number of pH swings [14]. For example, at 5 times pH swing, a 3 % anatase phase was formed for the pH Fle method calcined at

650°C, whereas a 75 % anatase phase was obtained for 20 times pH swings at the same calcination temperature. However, an 85 % anatase phase was observed in TiO_2 photocatalysts prepared by the pH Fix method at 800°C calcination up to 10 times pH swings. Thus, the pH Fix method could retain the anatase phase of the TiO_2 catalysts, irrespective of an increase in the number of pH swings and the calcination temperature, a significant observation of this study. The formation of the rutile phase for TiO_2 was observed only after 750°C calcination for pH Fix, as shown in Table 3.1. Photocatalysts prepared by the pH Fle method was reported to retain more of the anatase phase up to 600°C and 30 times pH swing [14], whereupon the anatase phase of TiO_2 changed to the rutile phase. When the catalysts were subjected to calcination above 600°C with the pH Fix method, a more anatase phase became evident up to a temperature of 750°C with up to 15 times pH swing (Table 3.1).

The particle size of the TiO_2 photocatalysts prepared by both methods increased with an increase in the number of pH swings (Fig. 3.2 and Table 3.1). This is due to the alternate addition of acid $TiCl_4$ and base aqueous ammonia during preparation of the TiO_2 catalysts at each swing time, in which small particles were dissolved by the acid solution and only large particles with high surface areas were retained. However, the average particle size of the catalysts prepared by pH Fix was found to be less than that by pH Fle,

as shown in Fig. 3.2. This is due to the dissolution of not only the smaller particles but also the large particles of TiO_2 by the high concentration of the HCl acid, resulting in the formation of only small TiO_2 particles with pH Fix. For pH Fle, the pH of the reaction mixture gradually became neutral when the number of pH swings increased to around 15 times. The effect of acid and alkaline was not very pronounced with pH Fle after a certain amount of pH swings, i.e., after a neutral pH was attained, however, the particles grew steadily with an increase in the pH swing numbers. It is worth noting that the surface area of the TiO_2 particles prepared by the pH Fle method increased with an increase in the pH swing numbers [Fig. 3.3], whereas, the reverse trend was observed for TiO_2 prepared by the pH Fix method. Although the particle size gradually increased with an increase in pH swings for both methods, not much influence was observed on the surface area for the particles prepared by pH Fix. This may be due to the existence of a small particle pore size and pore volume as well as the formation of a rutile phase at higher calcination temperatures. The rutile particles are aggregated larger particles responsible for a decrease in the surface area at higher calcination temperatures (Table 3.1), while at the same time, the pore volume and pore diameter have a strong influence on the morphology of the TiO_2 particles. Figures 3.4 and 3.5 clearly show that both the pore volume and pore diameter of the TiO_2 particles increased tremendously with an increase in the pH swing numbers with

the pH Fle method, whereas, only a slight increase in the pore volume and diameter of the TiO_2 particles were observed for the pH Fix method. The high pore volume and pore diameter of the particles were, thus, seen to be responsible for the high surface area of the particles prepared by pH Fle and the smaller pore volume and pore diameter were attributed to the smaller surface area of TiO_2 particles prepared by pH Fix. Well-crystalline TiO_2 particles were formed when the number of pH swings increased from 5 to 30. This is also another reason for the decrease in the surface area of TiO_2 particles prepared by the pH Fix method (Fig. 3.3).

The results of 2-propanol oxidation were investigated for the photocatalytic degradation ability of the catalysts prepared by these two methods and the results are shown in Fig. 3.6. The photocatalytic activity of the TiO_2 catalysts prepared by 20 times pH swings and calcined at 650°C showed a higher rate for the degradation of 2-propanol in comparison with other catalysts prepared by pH Fle with different pH swing numbers and calcination temperatures. Similarly, the catalysts prepared by 25 and 30 pH swing times and calcined at 650°C showed high activity for the degradation of 2-propanol using the pH Fix method, although it was still found to be less than the catalysts prepared by the pH Fle method, as shown in Fig. 3.6. A combination of both anatase and rutile phases have been reported to enhance the reaction rate for the degradation of organic pollutants to a

certain extent [17-19]. In this study, the catalysts prepared by 15 pH swing times by pH Fix and calcined at 750°C possessed a mixture of anatase and rutile phases in a ratio similar to the P-25 catalyst (Table 3.1). However, the catalytic activity was found to be less than the catalysts prepared by 30 times pH swings and calcined at 650°C which consisted of 94 % anatase. With pH Fle, the catalysts calcined at 650°C possessed an anatase/rutile ratio of around 75/25 with high pore volume and pore diameter, showing a high efficiency for the degradation of 2-propanol (78 %) (Fig. 3.6 and Table 3.2). The TiO_2 catalysts possessing an anatase/rutile ratio of around 70/30, with less pore volume and pore diameter than the catalysts prepared by 20 times pH swings, did not show high activity for the degradation of 2-propanol (58 %) (Table 3.2). Moreover, less pore volume and pore diameter were observed for the catalysts prepared with 5 times pH swings than with 20 times pH swings (Table 3.2). An anatase/rutile ratio of around 70/30, thus, had no effect on the photocatalytic activity for the degradation of organic compounds. This is clearly shown in Table 3.2 in which TiO_2 particles with a high pore volume and pore diameter showed excellent activity for the degradation of 2-propanol. These results reveal not only that the anatase/rutile phase is an important parameter for the catalytic reactions but also that other important parameters such as pore volume and pore diameter are equally important for the photocatalytic degradation reactions. The pH Fle method enabled

the preparation of more efficient TiO_2 photocatalysts comparable to P-25 (Fig. 3.6) than the pH Fix method, especially for photocatalytic degradation reactions as well as control of the morphology of the particles. With pH Fix, the particle size increased at a calcination temperature of 750ºC (Table 3.1), although the surface area did not increase proportionally and the pore size as well as pore volume were found to be less than the catalysts calcined at 650 and 700ºC. These results indicate that in addition to the anatase/rutile phase ratio, the particle size and surface area of the particles, and the pore volume and pore diameter are major factors in realizing the efficient photocatalytic degradation of organic compounds.

3.4. Conclusions

TiO_2 photocatalysts prepared by a controlled pH swing method could retain the anatase phase even at calcination temperatures of 750°C at high pH swing numbers. However, other important parameters such as particle size, surface area, pore volume, pore size as well as the anatase/rutile phase ratio could not be controlled well by this method. The addition of HCl acid during preparation showed detrimental effects on the morphology of the particles. On the other hand, TiO_2 catalysts prepared by an uncontrolled pH swing method showed better performance, especially in the control of such important parameters.

The results of 2-propanol oxidation showed that control of the anatase/rutile ratio, the pore volume as well as pore diameter of the TiO_2 nano-particles are important factors in realizing the efficient photocatalytic degradation of organic compounds.

Table 3.1.

Physicochemical properties of TiO_2 photocatalysts prepared by the fixed pH method

Calcination temperature (°C)	Number of pH swings	Surface area (m^2/g)	Particle size (nm)	Anatase:rutile	Pore volume (cc/g)	Pore diameter (nm)
700	15	31	14	93:07	0.139	19
700	20	32	18	90:10	0.151	20
700	25	33	20	89:11	0.154	21
700	30	38	22	93:07	0.200	23
750	15	20	19	85:15	0.102	22
750	20	16	25	55:45	0.099	24
750	25	15	26	60:40	0.066	25
750	30	15	27	50:50	0.100	26

Table 3.2.

Physicochemical properties of TiO_2 photocatalysts prepared by the flexible pH method

Number of pH swings	Calcination temperature (ºC)	Anatase:rutile	Pore-volume (cc/g)	Pore-diameter (nm)	2-propanol degradation (%)
5	550	70:30	0.135	13	58
10	600	60:40	0.293	31	64
15	650	67:33	0.515	57	77
20	650	75:25	0.513	64	78

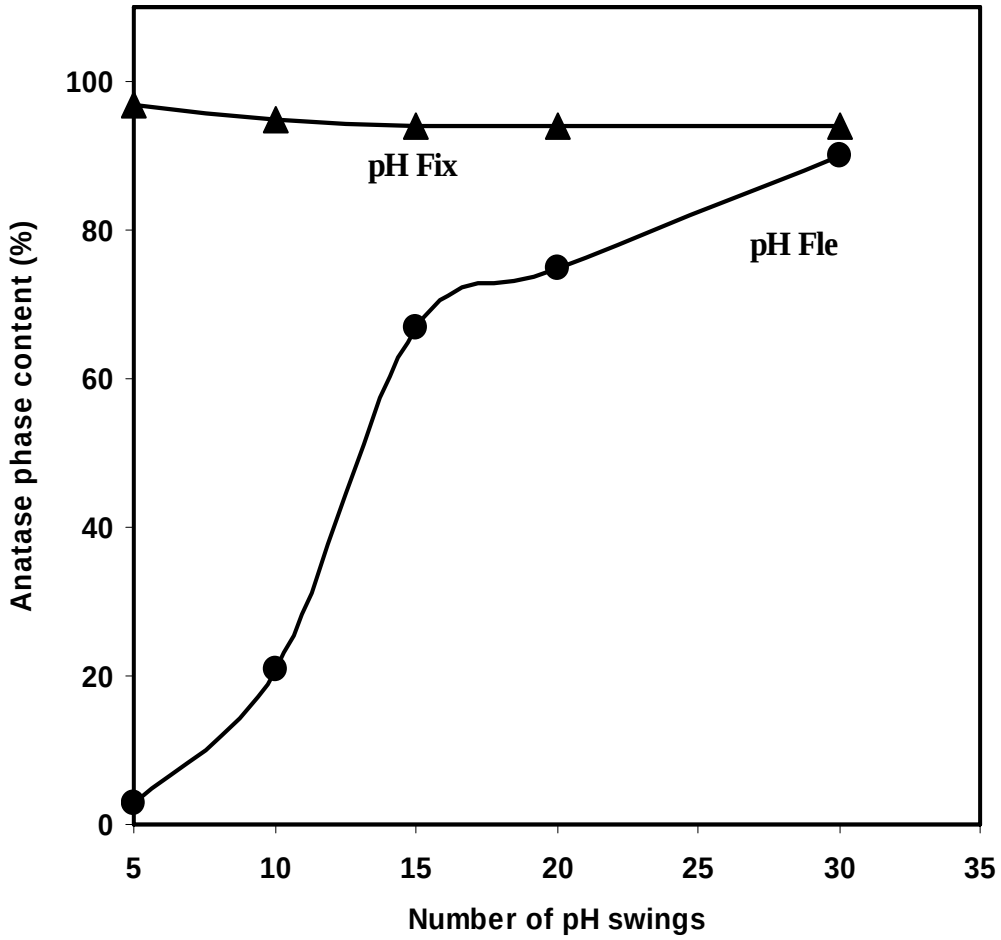

Figure 3.1. Effect of the number of pH swings on the anatase phase content of TiO_2 particles calcined at 650°C when prepared by the flexible (pH Fle) and fixed pH swing (pH Fix) methods.

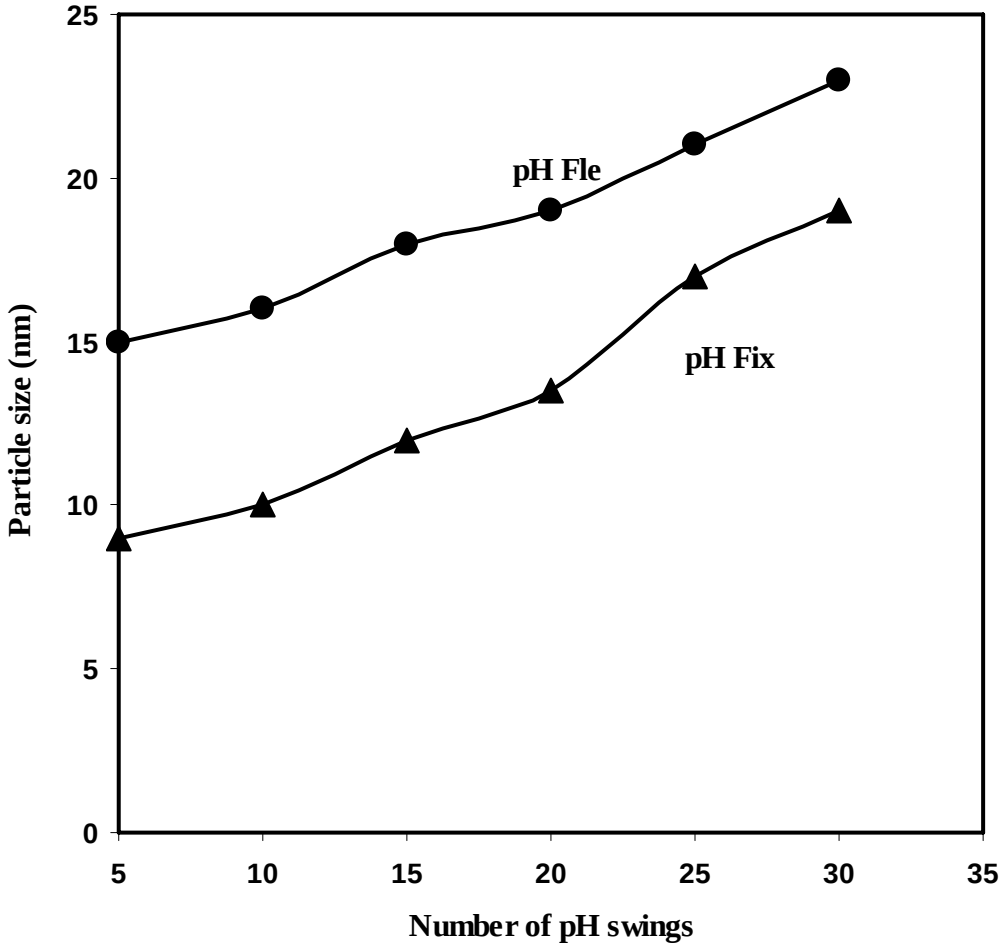

Figure 3.2. Particle size of photocatalysts calcined at 650°C versus the number of pH swings prepared by the flexible (pH Fle) and fixed pH swing (pH Fix) methods.

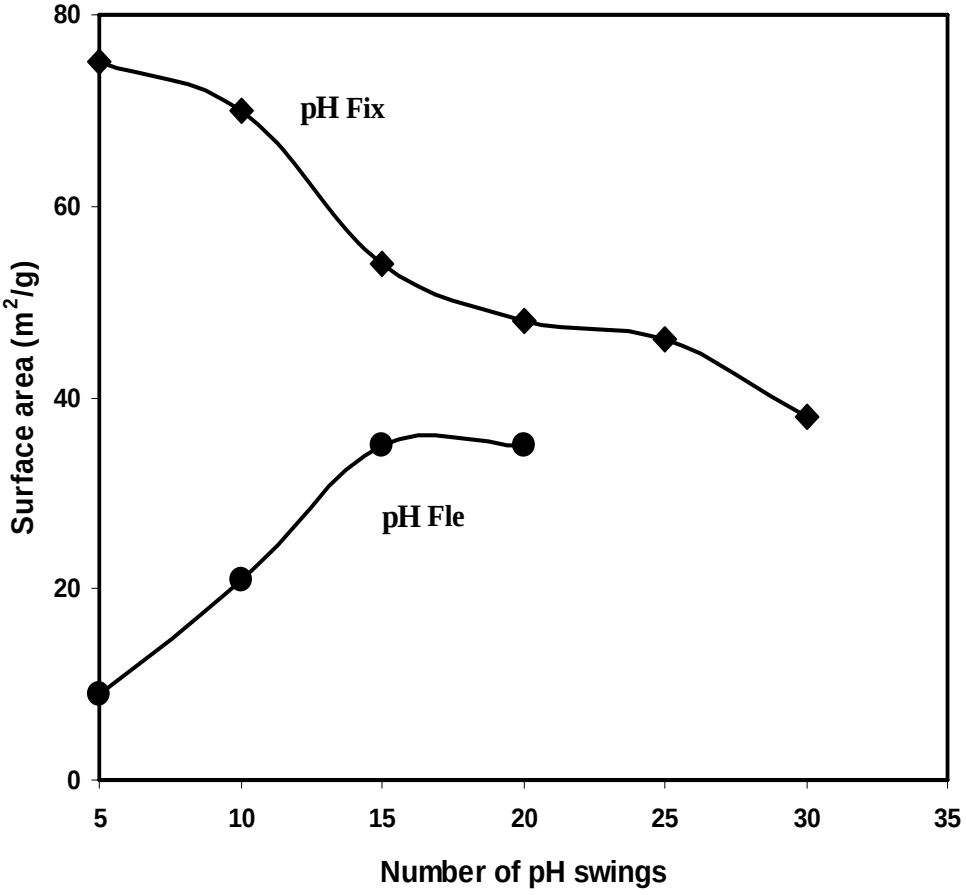

Figure 3.3. Specific surface area of photocatalysts calcined at 650°C versus the number of pH swings prepared by the flexible (pH Fle) and fixed pH swing (pH Fix) methods.

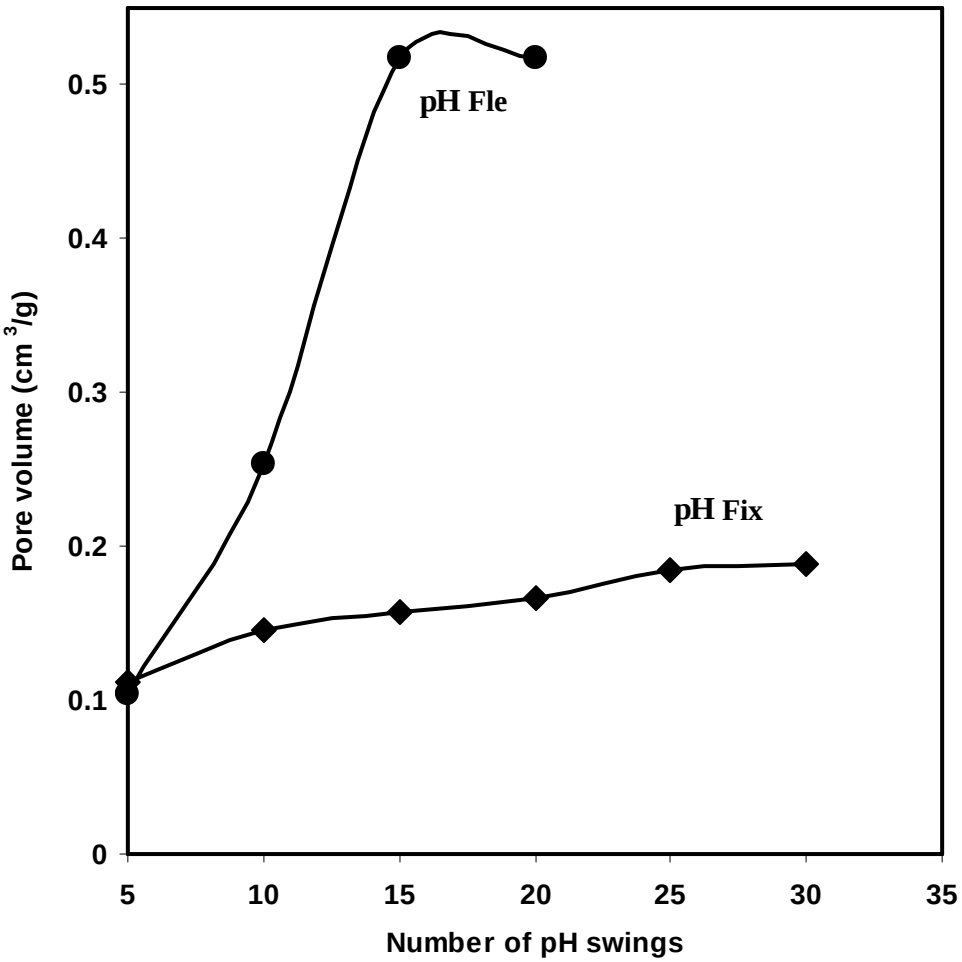

Figure 3.4. Pore-volume of photocatalysts calcined at 650°C versus the number of pH swings prepared by the flexible (pH Fle) and fixed pH swing (pH Fix) methods.

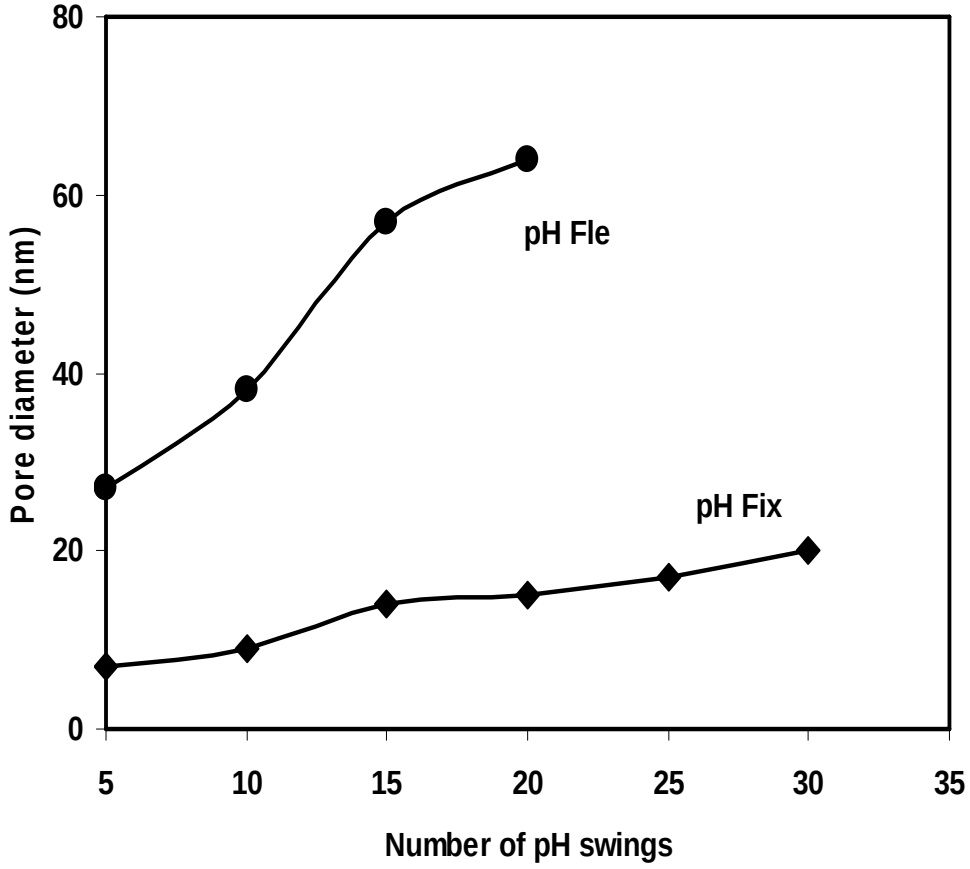

Figure 3.5. Pore-diameter of photocatalysts calcined at 650°C versus the number of pH swings prepared by the flexible (pH Fle) and fixed pH swing (pH Fix) methods.

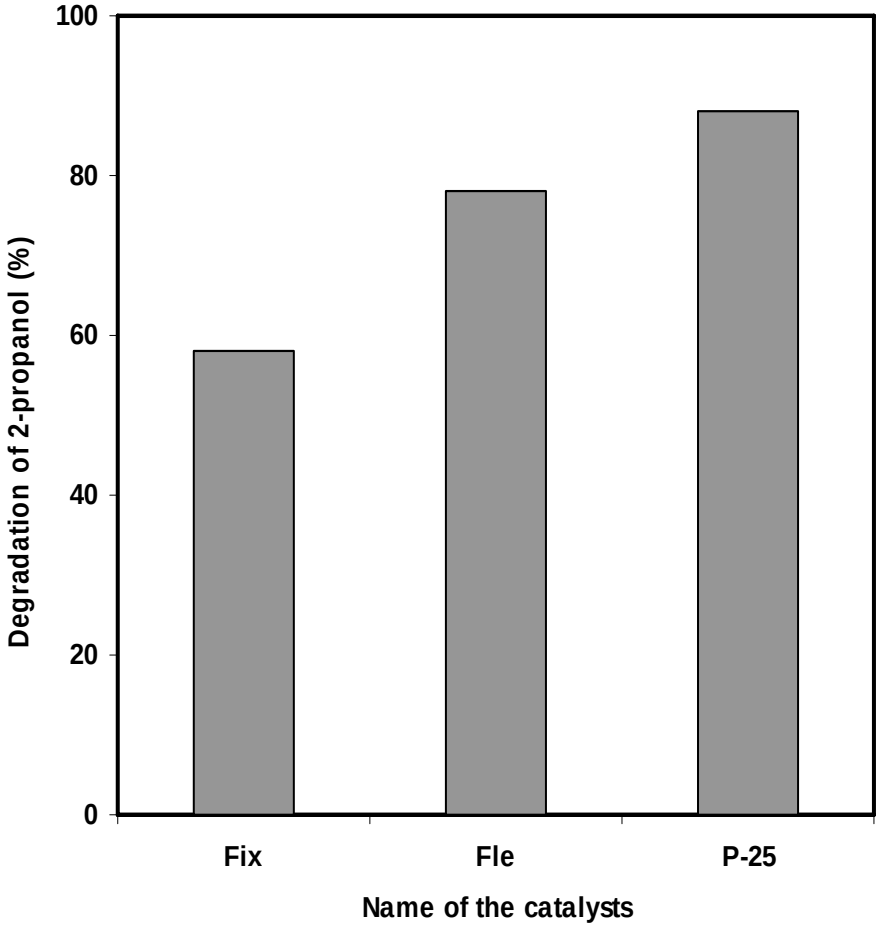

Figure 3.6. Comparison of the oxidative degradation of 2-propanol into CO_2 and H_2O (UV irradiation for 4 hrs at 297 K) using catalysts prepared by the flexible (pH Fle) & fixed pH swing (pH Fix) methods and P-25 TiO_2.

3.5. References

[1] M. Anpo, Bull. Chem. Soc. Jpn. **77,** 1427 (2004), and references therein.

[2] J. M. Herrmann, C. Guillard, J. Disdier, C. Lehaut, S. Malato and J. Blanco, Appl. Catal. B: Environmental, **35**, 281 (2002).

[3] C. Y. Wang, J. Rabani, D. W. Bahnemann and J. K. Dohrmann, J. Photochem. Photobiol. A Chem. **148**, 169 (2002).

[4] C. Morterra, G. Cerrato, M. Visca and D. M. Lenti, J. Mater. Chem. **2**, 341 (1992).

[5] M. Matsuoka, M. Kitano, M. Takeuchi, M. Anpo and J. M. Thomas, Topics Catal. **35**, 305 (2005).

[6] N. G. Park, J. V. D. Lagemaat and A. J. Frank, J. Phys. Chem. B, **104**, 8989 (2000).

[7] X. Z. Le, H. Liu, L. F. Cheng and H. J. Tong, Environ. Sci. Technol., **37**, 3989 (2003).

[8] Y. V. Kolenko, B. R. Churagulov, M. Kunst, L. Mazerolles and C. C. Justin, Appl. Catal. B: Environmental, **54**, 51 (200).

[9] S. Bakardjieva, J. Subrt, V. Stengl, M. J. Dianez and M. J. Sayagues, Appl. Catal. B: Environmental, **58**, 193 (2005).

[10] G. Q. Guo, J. K. Whitesell and M. A. Fox, J. Phys. Chem. B, **109**, 18781 (2005).

[11] H. Yamashita, Y. Ichihashi, M. Harada, G. Stewart, M. A. Fox and M. Anpo, J. Catal. **158** (1996) 97.

[12] M. Anpo and H. Yamashita, Catal. Surv. Asia **8**, 35 (2004), and references therein.

[13] M. Anpo and M. Takeuchi, J. Catal. **216**, 505 (2003).

[14] B. Neppolian, H. Yamashita, Y. Okada, H. Nishijima and M. Anpo, Catal. Lett. **105,** 111 (2005).

[15] J. F. Zhu, J. L. Zhang, F. Chen, K. Iino and M. Anpo, Topics Catal. **35**, 261 (2005).

[16] B. Neppolian, H. S. Jie, J. P. Ahn, J. K. Park and M. Anpo, Chem. Lett. **33**, 1562 (2004).

[17] D. C. Hurum, A. G. Agrios, K. A. Gray, T. Rajh and M. C. Thurnauer, J. Phys. Chem. B, **107**, 4545 (2003) .

[18] T. Ohno, K. Tokieda, S. Higashida and M. Matsumura, Appl. Catal. A: General, **244**, 383 (2003).

[19] T. Ohno, K. Sarukawa and M. Matsumura, J. Phys. Chem. B, **105**, 2417 (2001).

Chapter 4

Enhancement of the Photocatalytic Reactivity of TiO_2 Nano-particles by Simple Mechanical Blending with Hydrophobic MOR Zeolites

4. Enhancement of the Photocatalytic Reactivity of TiO_2 Nano-particles by Simple Mechanical Blending with Hydrophobic MOR Zeolites

4.1. Introduction

TiO_2 photocatalysts have been widely studied for the purification of air, water, and soil polluted with organic compounds for their potential to completely decompose harmful organic compounds into CO_2 and H_2O under UV light irradiation.[1-4] Various air-cleaning and deodorization systems equipped with TiO_2 photocatalysts and UV light sources that reduce volatile organic compounds (VOCs) such as aldehydes, carboxylic acids and aromatic compounds which can cause the so-called “sick house syndrome” are now commercially available. However, the removal efficiencies of air-cleaning systems for odorant compounds in the home environment still needs improvement, preferably by as simple and low-cost a method as possible. Although the deposition of small amounts of Pt on TiO_2 catalyst surfaces is generally known to enhance the photocatalytic reactivity,[5-9] Pt compounds are too costly for common use in home electrical appliances. On the other hand, the hybridization of adsorbents such as zeolites [10-12] and activated carbon [13-15] with TiO_2 particles has been reported to show elevated photocatalytic reactivity, especially for the decomposition of gaseous organic compounds. In a previous report,[16] we have

shown that hybridized TiO_2/MOR catalysts prepared by a simple impregnation method also exhibit high photocatalytic reactivity for the complete oxidation of gaseous acetaldehyde as compared to pure untreated TiO_2 catalysts since MOR zeolite powders are able to efficiently adsorb acetaldehyde molecules diffused in wide spaces and then smoothly supply them onto the TiO_2 photocatalyst surfaces.

In this work, TiO_2 nano-particles were mechanically blended with the hydrophobic MOR zeolite in a simple preparation method in order to maximize the photocatalytic performance of commercial TiO_2 powders as well as reduce the preparation cost. The photocatalytic reactivity of the blended TiO_2/MOR systems were then evaluated for the complete oxidation of gaseous acetaldehyde with O_2 under UV light irradiation.

4.2. Experimental

TiO_2 nano-powdered photocatalysts (SSP-25, anatase phase, SSA_{BET} = ca. 270 m^2/g) and the highly siliceous H^+-type MOR zeolite (HSZ-HOA890, SiO_2/Al_2O_3 = ca. 1880, SSA_{BET} = ca. 370 m^2/g) were purchased from Sakai Chemical Industry Co., Ltd. and Tosoh Co., Ltd., respectively. TiO_2/MOR photocatalysts having different TiO_2 content were obtained by a simple mechanical blending of these two powder samples in an agate mortar for 0 - 60 min [referred to as TiO_2/MOR(A)]. For comparison, a different type of

TiO_2/MOR photocatalysts was also prepared by the ultrasonic aqueous suspension of these two powder samples [referred to as TiO_2/MOR(B)]. The TiO_2 nano-powders blended with the MOR zeolites were then characterized by XRD (Shimadzu, XRD-6100) and diffuse reflectance UV-vis absorption (Shimadzu, UV-2200A) measurements at room temperature.

The photocatalytic reactivity of the blended TiO_2/MOR samples was evaluated for the decomposition of gaseous acetaldehyde in the presence of O_2 under UV light irradiation. The TiO_2/MOR catalysts (50 mg) were placed onto a flat bottom quartz cell (volume, ca. 33 cm^3). The volume of the reaction area including the cell volume was ca. 100 cm^3. Before photoreactions were carried out, the catalysts were degassed at 723 K for 2 h, treated in sufficient amounts of O_2 (ca. 6.7 kPa) at the same temperature for 2 h, and then degassed at 373 K for 2 h up to a 10^{-5} kPa range. A gas mixture of CH_3CHO (0.27 kPa), O_2 (1.07 kPa), and H_2O (0 - 1.33 kPa) was then introduced into the reaction cell. The amount of acetaldehyde introduced into the reaction cell was calculated as ca. 8 μmol (ca. 1500 ppm). After an adsorption equilibrium was reached, UV light was irradiated at 275 K by a 100 W high-pressure Hg lamp (Toshiba, SHL-100UVQ-2) through a cutoff filter (Toshiba Glass, UV-27, λ>270 nm, ca. 1-2 mW/cm^2). To avoid the heating effect from the UV lamp, the photocatalysts in the quartz cell were cooled in ice water during the photoreactions. The amount of CO_2 produced and acetaldehyde decomposed were analyzed by TCD and

FID by gas chromatography (Shimadzu, GC-14A).

4.3. Results and Discussion

Figure 4.1 shows the XRD patterns of the TiO_2 nano-powders blended with MOR zeolites of different TiO_2 contents. The TiO_2 nano-powders showed typical diffraction patterns attributed to the (101) phase of an anatase structure at around 26 degrees. The primary particle size of the TiO_2 nano-powder (SSP-25) could be estimated at ca. 8 nm by the Scherre's equation. On the other hand, all diffraction patterns for the MOR zeolite which could be assigned to a MFI structure much sharper than the TiO_2 nano-powder, showing largely grown zeolite crystals. When small amounts of TiO_2 nano-powders were mechanically blended with such largely grown zeolite particles even for only 5 min, it became difficult to observe the diffraction patterns attributed to the TiO_2 nano-powders. However, as the TiO_2 content increased up to 20 wt%, a broad diffraction peak attributed to the anatase (101) phase could be observed at around 26 degrees.

The diffuse reflectance UV-vis absorption spectra of the TiO_2 nano-particles mechanically blended with the siliceous MOR zeolite and non-porous pure SiO_2 powder are shown in Figs. 4.2-A and 4.2-B, respectively. The absorption edges of the TiO_2

nano-powders blended with the MOR zeolites were observed at around 380 - 400 nm. When smaller amounts of TiO_2 powders than 5 wt% were blended with the siliceous MOR or SiO_2 powders, some portion of the incident light was found to pass through the powder samples of several millimeters thickness due to the high transparency of the MOR and SiO_2 powders. When the amount of TiO_2 nano-powders blended with the zeolite powders reached about 10 - 20 wt%, the incident light could not penetrate the mixed powder samples, suggesting efficient irradiation of UV light onto the entire TiO_2 nano-particles. However, since the absorption coefficient of the TiO_2 powder in UV light regions is known to be very high, as the fraction of the TiO_2 powders to the zeolite powders increased, the incident light could not be irradiated onto the backside of the TiO_2 particles. These results clearly indicate that an important role of the siliceous MOR zeolite or SiO_2 powders is the efficient irradiation of incident UV light onto all of the TiO_2 nano-particles without any loss of light intensity.

The oxidation of gaseous acetaldehyde on TiO_2 photocatalysts hardly proceeded in the absence of a H_2O vapor, however, the photocatalytic reaction was dramatically enhanced by adding small amounts of H_2O vapor [16]. The photocatalytic oxidation reactions of gaseous acetaldehyde with O_2 under UV light irradiation (λ>270 nm) over the TiO_2 nano-particles blended with the hydrophobic MOR zeolite (SiO_2/Al_2O_3 = 1880) were, thus,

evaluated in the presence of a H_2O vapor. At first, the effect of the mechanical mixing times of these two different powder samples on the photocatalytic reactivity of TiO_2/MOR(A) was evaluated from the viewpoint of the dispersion of the TiO_2 nano-particles within the zeolite powders. As shown in Fig. 4.3, although the increased dispersion of the TiO_2 nano-particles onto the powders after mixing up to 60 min could be confirmed by SEM observations (not shown), the photocatalytic reactivity could hardly be enhanced. For comparison, the mixed TiO_2/MOR(B) powders were prepared from an ultrasonically aqueous suspension. However, as shown in Fig. 4.4, the photocatalytic reactivity of TiO_2/MOR(B) was almost equivalent to the TiO_2/MOR(A) prepared by a simple mechanical blending method. Moreover, it is notable that the TiO_2 and zeolite powders without mixing in an agate mortar showed slightly less photocatalytic reactivity as compared to the mechanically blended TiO_2/MOR(A). These results clearly indicate that the photocatalytic reactivity of the TiO_2 nano-particles is easily improved by simple mechanical blending with a hydrophobic zeolite powder as an adsorbent material.

Figure 4.5 shows the effects of the TiO_2 content on the photocatalytic reactivity of the mechanically blended TiO_2/MOR(A) for the complete oxidation of gaseous acetaldehyde with O_2 in the presence of H_2O vapor under UV light ($\lambda > 270$ nm) irradiation. TiO_2 nano-particles of ca. 5 - 15 wt% mechanically blended with the siliceous MOR zeolite of

hydrophobic character showed almost twice as high photocatalytic reactivity as compared to the pure untreated TiO_2 nano-particles. Also, as reported in a previous work, the siliceous MOR zeolite can work as a good adsorbent to concentrate gaseous acetaldehyde in hydrophobic cavities.[16] Since the siliceous zeolite does not have Brönsted acid sites, which work as strong adsorption sites for polar molecules such as H_2O molecules,[17] the acetaldehyde molecules concentrated within the zeolite cavities could smoothly diffuse on the catalyst surfaces. In addition, as mentioned from the results of UV-vis absorption measurements, the incident UV light was efficiently irradiated on the entire TiO_2 photocatalyst of ca. 5 - 15 wt% blended with the MOR zeolite due to the high transparency of the zeolite powders in UV-vis light regions. In order to verify the role of the zeolite powders, the photocatalytic reactivity of the TiO_2 nano-particles mechanically blended with non-porous silica powders were also investigated. Although the non-porous silica (SSA_{BET} = less than 10 m^2/g) adsorbed only small amounts of gaseous acetaldehyde molecules as compared to the MOR zeolite, transparent silica powders can work as an efficient diluting material for the TiO_2 nano-particles. In this case, the non-porous silica powders did not show any condensation effect for the acetaldehyde molecules. Small amounts of the TiO_2 nano-particles blended with the non-porous silica powders, thus, showed low photocatalytic reactivity. From these results, the critical role of the

hydrophobic MOR zeolite to enhance the photocatalytic reactivity of TiO_2 nano-particles can be concluded to be: (i) the condensation effect for gaseous acetaldehyde molecules near the TiO_2 photocatalytic sites; and (ii) the appropriate diluent effect of the TiO_2 photocatalysts as an intense absorber of UV light with highly transparent zeolite powders.

For further verification of the condensation of gaseous acetaldehyde molecules, the photocatalytic oxidation reaction of different initial concentrations of acetaldehyde over the TiO_2 nano-particles and TiO_2/MOR(A) were compared. As shown in Fig. 4.6, when only TiO_2 nano-particles were applied for the photocatalytic oxidation of gaseous acetaldehyde, the total conversion of acetaldehyde into CO_2 and H_2O was found to decrease with a decrease in the initial pressure of acetaldehyde. On the other hand, TiO_2 nano-particles mechanically blended with the hydrophobic zeolite powders were found to show high and efficient photocatalytic reactivity for rather lower concentrations of acetaldehyde molecules. These results clearly indicate that the non-porous TiO_2 nano-powders cannot condense low concentrations of gaseous acetaldehyde molecules on their surfaces in spite of their large surface area (ca. 270 m^2/g), while the acetaldehyde molecules concentrated within the hydrophobic cavities of the MOR zeolites quickly diffused onto the TiO_2 nano-particles, resulting in the efficient photocatalytic oxidation of acetaldehyde into CO_2 and H_2O under UV light irradiation. Since the concentration of

gaseous acetaldehyde from home environments is generally at most 50 ppm, TiO_2 nano-particles mechanically blended with MOR zeolite powders are good candidates for the continuous removal of lower and more dilute concentrations of harmful organic compounds.

4.4. Conclusions

The photocatalytic properties of conventional TiO_2 nano-particles (SSP-25, Sakai Chemical Industry Co., Ltd.) could be enhanced by simple mechanical blending with hydrophobic MOR zeolite powders. The optimum amount of the zeolite powders as an adsorbent for the enhancement of the photocatalytic reactivity of the blended TiO_2/MOR system was estimated to be ca. 80 - 95 wt% since the incident UV light was effectively irradiated onto the entire TiO_2 nano-particles due to the high transparency of the siliceous zeolite powders. Furthermore, the hydrophobic zeolite powders efficiently gathered the gaseous acetaldehyde molecules within their cavities and supplied them onto the TiO_2 surfaces, resulting in an enhancement of the photocatalytic reactivity.

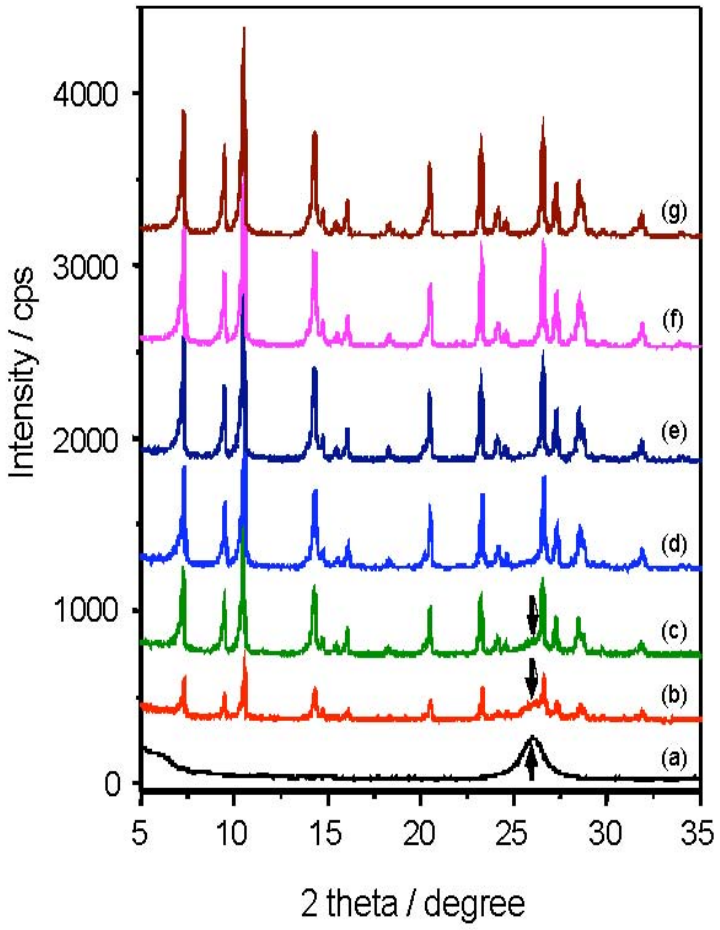

Figure 4.1. XRD patterns of TiO_2 nano-particles mechanically blended with MOR (SiO_2/Al_2O_3 = 1880) zeolite powders.

TiO_2 content (wt%): (a) 100, (b) 50, (c) 20, (d) 10, (e) 5, (f) 1, and (g) 0.

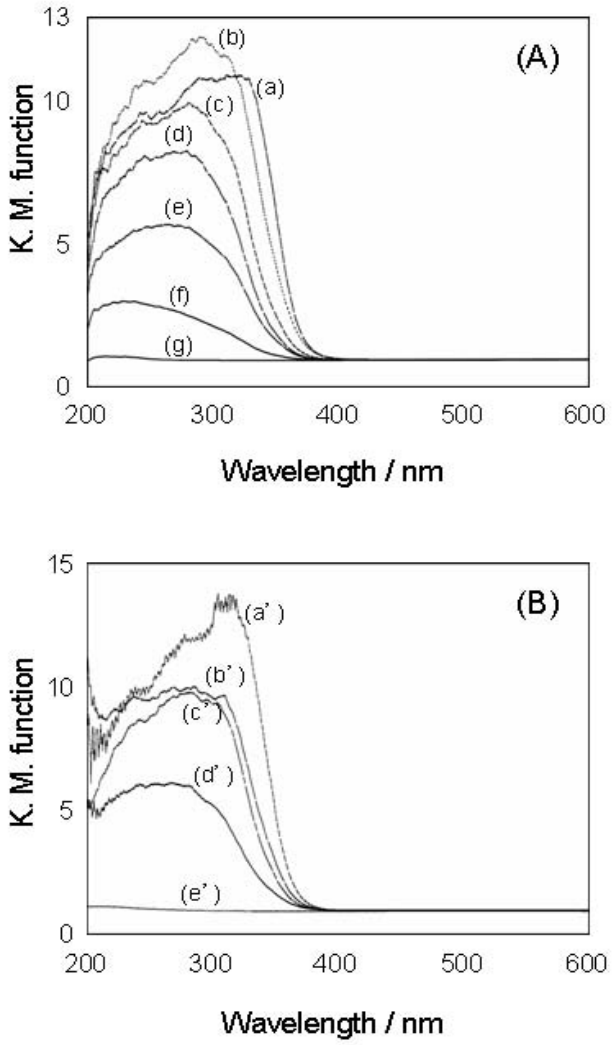

Figure 4.2-A Diffuse reflectance UV-Vis absorption spectra of TiO_2 nano-particles mechanically blended with MOR zeolite powders.

TiO_2 content (wt%): (a) 100, (b) 50, (c) 20, (d) 10, (e) 5, (f) 1, and (g) 0.

Figure 4.2-B Diffuse reflectance UV-Vis absorption spectra of TiO_2 nano-particles mechanically blended with non-porous pure SiO_2 powders.

TiO_2 content (wt%): (a') 100, (b') 50, (c') 20, (d') 5, (e) 0.

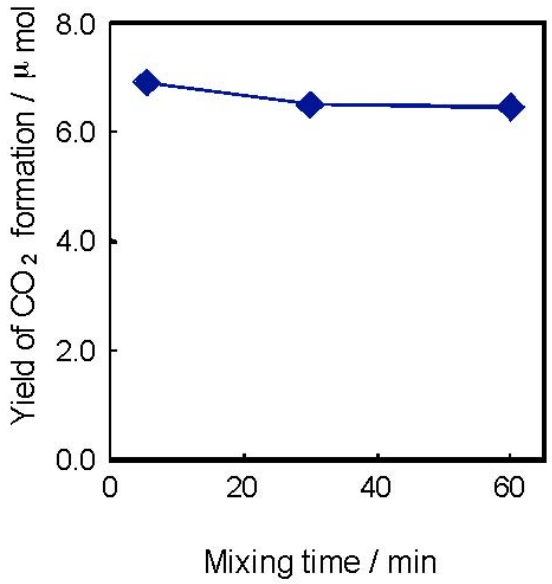

Figure 4.3 Effect of the mixing time for the TiO_2 and zeolite powders (TiO_2/MOR ratio = 10/90) in an agate mortar on the photocatalytic reactivity for the oxidation of gaseous acetaldehyde with O_2 under UV light irradiation.

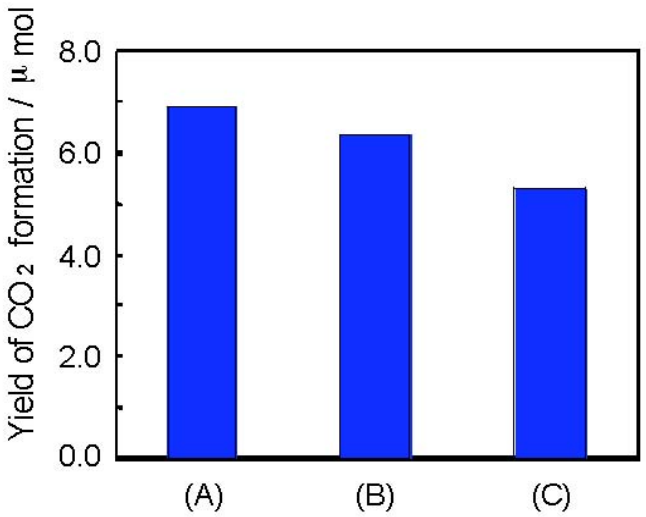

Figure 4.4 Photocatalytic reactivity (UV light irradiation: 1 h) of the blended TiO_2/MOR samples (TiO_2/MOR ratio = 10/90) prepared by: (A) mechanical blending, (B) an ultrasonically aqueous suspension, and (C) without mixing.

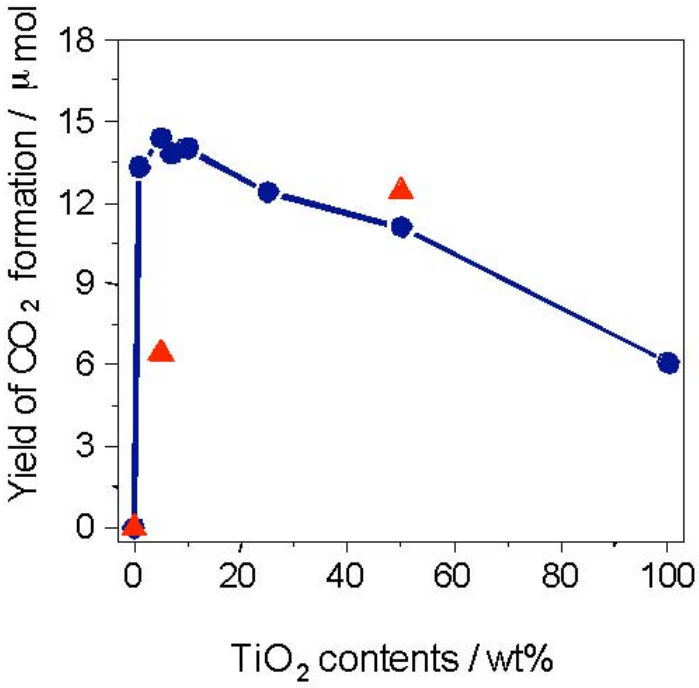

Figure 4.5 Photocatalytic reactivity (UV light irradiation: 3 h) of the TiO_2 nano-particles mechanically blended with MOR and the non-porous SiO_2 powder samples.

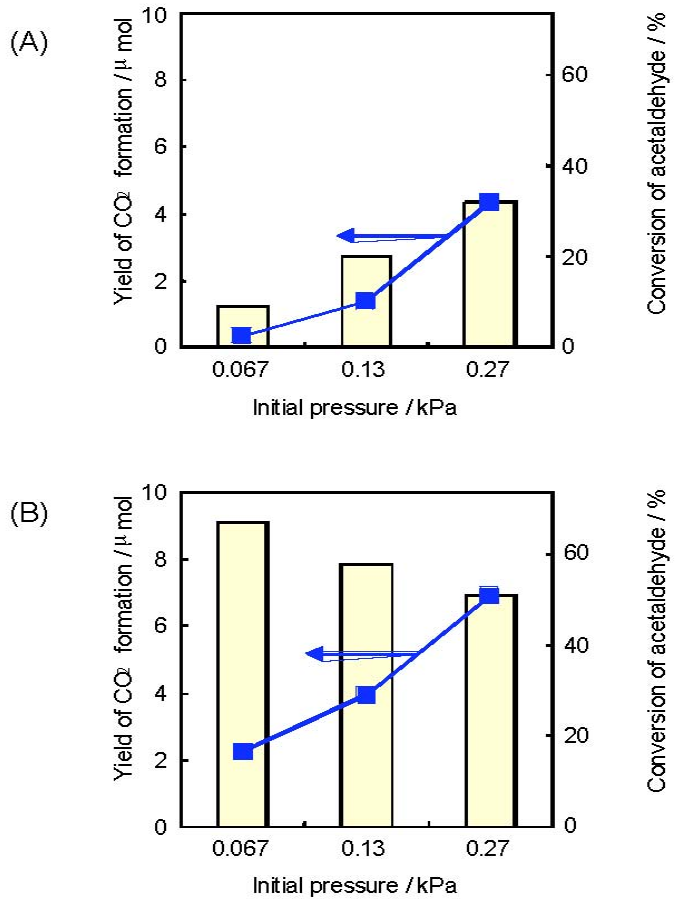

Figure 4.6 Effect of different initial pressures of acetaldehyde on the photocatalytic reactivity of: (A) the TiO_2 nano-particles, and (B) the TiO_2 nano-particles mechanically blended with the MOR zeolite powders (TiO_2/MOR ratio = 5/95).

4.5. References

[1] N. Serpone, E. Pelizzetti (Eds.), "Photocatalysis fundamentals and applications", Wiley, New York (1989).

[2] D.F. Ollis, H. Al-Ekabi (Eds.), "Photocatalytic Purification and Treatment of Water and Air", Elsevier, Amsterdam (1993).

[3] A. Fujishima, K. Hashimoto, T. Watanabe (Eds.), "TiO_2 Photocatalysis Fundamentals and Applications", BKC, Tokyo (1999).

[4] M. Anpo, H. Yamashita, in: M. Schiavello (Ed.), "Heterogeneous Catalysis", Wiley, London (1997).

[5] S. Sato and J. M. White, Chem. Phys. Lett. 72, 83 (1980).

[6] M. Grätzel (Ed.), "Energy Resources through Photochemistry and Catalysis" Academic Press, New York (1983).

[7] M. Anpo, T. Shima, S. Kodama, Y. Kubokawa, J. Phys. Chem. 91, 4305 (1987).

[8] M. Anpo, K. Chiba, M. Tomonari, S. Coluccia, M. Che, M. A. Fax, Bull. Chem. Soc. Jpn. 64, 543 (1991).

[9] M. Takeuchi, K. Tsujimaru, K. Sakamoto, M. Matsuoka, H. Yamashita, M. Anpo, Res. Chem. Intermed., 29, 6, 619 (2003).

[10] N. Takeda, T. Torimoto, S. Sampath, S. Kuwabata, H. Yoneyama, J. Phys. Chem. 99,

9986 (1995).

[11] V. Durgakumari, M. Subrahmanyam, K.V. Subba Rao, A. Ratnamala, M. Noorjahan, K. Tanaka, Appl. Catal. A Gen. 234 (2002) 155.

[12] M. Anpo (Ed.), "Photofunctional Zeolites", NOVA, New York (2000).

[13] T. Ibusuki, K. Takeuchi, J. Mol. Catal. 88, 93 (1994).

[14] H. Uchida, S. Itoh, H. Yoneyama, Chem. Lett. 1995 (1993).

[15] H. Yamashita, M. Harada, A. Tanii, M. Honda, M. Takeuchi, Y. Ichihashi, M. Anpo, N. Iwamoto, N. Itoh, T. Hirao, Catal. Today 63, 63 (2000).

[16] M. Takeuchi, T. Kimura, M. Hidaka, D. Rakhmawaty, M. Anpo, J. Catal., 246, 235 (2007).

[17] N.Y. Chen, J. Phys. Chem. 80, 60 (1976).

Chapter 5

Preparation of the Visible Light Responsive TiO_2 Thin Film Photocatalysts by a RF-magnetron Sputtering Deposition Method

5. Preparation of Visible Light Responsive TiO_2 Thin Film Photocatalysts by a RF-magnetron Sputtering Deposition Method

5.1. Introduction

In recent years, TiO_2 photocatalysts have been intensively investigated in various fields and particularly TiO_2 thin films coated on various substrates have shown potential for applications as photofunctional materials not only for their high photocatalytic reactivity but also for their highly wettable properties under UV light irradiation [1-3]. Although various products using TiO_2 thin film photocatalysts have already been commercialized, they do not allow the absorption of visible light and, therefore, necessitates the use of a UV light source. However, in order to realize clean and safe chemical processes as well as the use of abundant solar energy, photocatalysts able to operate even under visible light irradiation are strongly desired. Since an important consideration for widespread and practical applications of high performing TiO_2 photocatalysts is the preparation cost, various methods such as the sol-gel [4-7], chemical vapor deposition (CVD) [8-10], and plasma-enhanced CVD methods [11-13] have been intensively investigated. Among these, the RF (radio frequency) magnetron sputtering deposition method described here was found to be suitable for practical applications since

it enables not only high speed deposition but also deposition of thin films on various substrates with large areas.

We have previously reported on metal ion-implantation into TiO_2 semiconductor powders and thin films, resulting in an effective modification of their electronic properties to enable the absorption of visible light [14-16]. However, this method necessitates two processes: (i) ionized cluster beam (ICB) deposition to prepare the transparent TiO_2 thin films; and (ii) modification of the electronic properties of the TiO_2 semiconductors by a highly advanced metal ion implantation procedure. Since such complexity in the preparation processes impedes mass production at low cost, much easier preparation methods for visible light responsive TiO_2 thin films are strongly desired in order to realize widespread applications.

In this paper, a more practical alternative preparation process, i. e., a RF magnetron sputtering (RF-MS) deposition method has been successfully applied for the development of transparent TiO_2 thin films which can induce various significant photocatalytic reactions effectively under UV and visible light irradiation.

5.2. Experimental

TiO_2 thin films were prepared by a RF magnetron sputtering deposition method.

Quartz substrates were ultrasonically cleaned in acetone for 15 min, dried at 373 K for half a day, and then calcined in air at 723 K for 5 h in order to obtain clean surfaces. Before deposition of the TiO_2 thin films, quartz substrates were degassed until less than 5 x 10^{-4} Pa (3.8 x 10^{-6} Torr) in a high vacuum chamber by a rotary pump and turbo molecular pump. A schematic diagram of this deposition method is shown in Fig. 5.1. The Ar^+ ions in the Ar gas plasma induced by the magnetic and electric fields sputter the TiO_2 target surfaces at high speed to produce sputtered ions such as Ti^{4+} and O^{2-}. These ions produced by the Ar gas plasma are accumulated onto the substrate surfaces to form TiO_2 thin films. In a conventional reactive sputtering method, oxide thin films are prepared by sputtering a metallic Ti target in the presence of O_2 atmosphere as the reactive gas. However, in this study, since a TiO_2 plate with a rutile structure (High Purity Chemicals Lab. Corp., grade: 99.99 %) was applied as the ion source material (sputtering target), only Ar was used as the sputtering gas without coexisting O_2 as the reactive gas. The physicochemical, mechanical and photocatalytic properties of the obtained TiO_2 thin films were strongly affected by the preparation conditions such as induced RF power, substrate temperature, distance between target and substrates (D_{TS}), and sputtering gas flow rate, etc. The induced RF power was adjusted to 300 W, the substrate temperatures were changed from 373 K to 973 K and D_{TS} was set at 80 mm. The flow rate of Ar gas was kept at 25 SCCM and the

pressure of the sputtering gas under deposition process was about 2.0 Pa (1.5 x 10^{-3} Torr). Since the TiO_2 thin films are deposited under high vacuum conditions, contamination with some impurities into TiO_2 thin films could be avoided. No post-calcination treatments were carried out. The film thicknesses of these thin films were controlled at ca. 1 μm by changing the deposition time.

Characterization of these TiO_2 thin films were carried out by XRD (Rigaku, RINT-1200) and UV-Vis absorption measurements (Shimadzu, UV-2200A). The surface morphologies of the thin films were investigated by SEM (Hitachi, S-4700) and AFM (Seiko Instruments, SPA300) analyses. Furthermore, their atomic compositions from top surface to deep bulk were investigated by AES measurements (ULVAC-PHI, SAM670).

The photocatalytic reactivities of the TiO_2 thin films were evaluated by carrying out the decomposition of NO under UV ($\lambda > 270$ nm) or visible ($\lambda > 450$ nm) light irradiation [14, 17]. Light irradiation was carried out using a conventional 100 W high-pressure Hg lamp (Toshiba, SHL-100UVQ-2) through cutoff (Toshiba Glass, UV-27 or Y-45) and water filters at 275 K. The reaction products were analyzed by a gas chromatograph equipped with a TCD detector.

5.3. Results and Discussion

The optical property is one of the most important factors determining the photocatalytic performance. Figure 5.2 shows the UV-Vis absorption (transmittance) spectra of the TiO_2 thin films prepared at different preparation temperatures. The TiO_2 thin films prepared at low temperatures ($T < 473$ K) showed high transparency and clear interference fringes in the visible light region, like TiO_2 thin films prepared by sol-gel [4-7] or ionized cluster beam (ICB) deposition [14, 17]. These results clearly indicate that stoichiometric and uniform TiO_2 thin films can be prepared by using a TiO_2 plate as the sputtering target and Ar as the sputtering gas without the coexistence of O_2 as the reactive gas. As the preparation temperatures increased, the TiO_2 thin films were found to show effective absorption in visible light regions with a maximum for the thin film deposited at 873 K. Since the amount of impurities included in the TiO_2 target material is very low (lower than 0.1 %), hardly any impurities were included in the deposited thin films. The TiO_2 thin films prepared by the sputtering TiO_2 target in the presence of O_2 at 873 K did not exhibit any significant absorption in visible light regions (data not shown). These results indicate that visible light-responsive TiO_2 thin films could successfully be prepared only when the TiO_2 target as the ion source is sputtered with Ar gas without the coexistence of O_2 gas at relatively high temperatures ($T > 773$ K).

The XRD patterns of the TiO_2 thin films prepared at different substrate temperatures

are shown in Fig. 5.3. The TiO_2 thin films prepared at temperatures lower than 673 K showed a specific diffraction peak at around 37.9 degrees attributed to the anatase (004) phase. Since a conventional TiO_2 powder (Degussa, P-25) does not show such an intense peak due to the (004) phase of the anatase structure, this (004) phase may be considered characteristic to the TiO_2 thin films prepared by this RF-MS deposition method. For the TiO_2 thin films prepared at 873 K, a diffraction peak at 25.4 degrees due to the anatase (101) phase was found to largely decrease, however, the (004) phase was relatively stable. The TiO_2 thin films readily able to absorb visible light were mainly composed of a rutile structure of for the TiO_2. As summarized in Table 5.1, the primary particle sizes of the anatase and rutile phases in the TiO_2 thin films were determined by using the Scherrer's equation from the diffraction peaks at ca. 25 and 28 degrees, respectively. The particle sizes of the TiO_2 which make up the thin films were not largely affected by the preparation temperatures and were constant at about 20 nm. Since thin films are generally strained by interfacial stress on the substrates, crystallization along their depth direction may be restricted.

The TiO_2 thin films prepared by the RF-MS deposition method were found to efficiently induce the photocatalytic decomposition of NO into N_2 and N_2O under UV light ($\lambda > 270$ nm) irradiation. Figure 5.4 shows the reaction time profiles for the

photocatalytic decomposition of NO over the TiO_2 thin film prepared at 473 K and a commercial TiO_2 powder (Degussa, P-25) under UV light irradiation. The transparent TiO_2 thin films prepared by the RF-MS method showed almost the same photocatalytic reactivity for the reductive decomposition of NO under UV light irradiation as TiO_2 powders known to be highly reactive photocatalysts. Figure 5.5 shows the effect of the preparation temperatures on the photocatalytic reactivity of the TiO_2 thin films for the decomposition of NO under UV light irradiation. The TiO_2 thin film prepared at 473 K showed the highest photocatalytic performance under UV light irradiation, however, as the preparation temperatures increased, the reactivity of the TiO_2 thin films decreased. These results can be explained by the observation that the TiO_2 thin films prepared at relatively lower temperatures are highly transparent and, thus, the incident UV light can pass through the thin films, resulting in effective utilization of the incident light to generate electron-hole pairs. However, since the thin film sample prepared at 373 K also included some amorphous phase which means a low crystallinity, this sample showed lower reactivity as compared to that prepared at 473 K. XRD measurements also revealed that the TiO_2 thin films prepared at lower temperatures mainly consist of an anatase structure, on the other hand, those prepared at relatively higher temperatures crystallize well to a rutile structure. These differences in the crystal structures of the TiO_2 thin films showed a

good correspondence with their photocatalytic reactivities under UV light irradiation.

The photocatalytic reactivities of these TiO_2 thin films under visible light irradiation ($\lambda > 450$ nm) were also investigated. As shown in Fig. 5.6, although the reference TiO_2 powder (Degussa, P-25) did not show any photocatalytic reactivity under visible light irradiation, the TiO_2 thin film photocatalyst prepared at 873 K was found to efficiently decompose NO into N_2 and N_2O even under visible light irradiation. Figure 5.7 shows the effects of the preparation temperatures on the photocatalytic reactivity under visible light irradiation as well as on the relative intensities at wavelengths of 450 nm in the UV-Vis absorption spectra, as shown in Fig. 5.2. As the preparation temperatures increased, the photocatalytic reactivity under visible light irradiation was found to increase as well, reaching a maximum at 873 K. However, the thin film sample prepared at 373 K showed rather low reactivity under visible light irradiation. Since this sample prepared at 373 K showed lower crystallinity as compared to that prepared at 473 K, some oxygen vacant sites may exist on the surface of the thin film samples and work as NO reductive sites. Moreover, the order of the photocatalytic reactivity under visible light irradiation corresponds well with the relative intensities at wavelengths of 450 nm in the UV-Vis absorption spectra. These results clearly indicate that the TiO_2 thin films prepared by a RF-MS method do, in fact, work as photocatalysts even under visible light irradiation of

wavelengths longer than 450 nm. However, since the semiconducting powder samples which absorb visible right do not always show photocatalytic reactivity under visible light irradiation, other factors to determine the photocatalytic performance, such as BET surface areas, surface roughness, oxygen vacancies which may work as recombination centers, also need to be investigated.

TiO_2 photocatalysts are also known to show the potential to completely oxidize various organic compounds into harmless CO_2 and H_2O under UV light irradiation [18-21]. These visible light-responsive TiO_2 thin films prepared by the RF-MS method were confirmed to be effective for other photocatalytic reactions as such as the complete oxidation of various organic compounds into CO_2 and H_2O as well as the splitting of H_2O into H_2 and O_2 under UV (λ> 270 nm) and visible light (λ> 450 nm) irradiation [22-25].

The mechanisms for the efficient absorption of visible light has been discussed from the viewpoint of the surface morphology and O/Ti ratios of the TiO_2 thin films prepared by the RF-MS method. Figure 5.8 shows the AFM images of the TiO_2 thin films prepared at 473 K and 873 K. The surface morphology and roughness of the films prepared at 873 K was found to be about three times higher than the films prepared at 473 K. Additionally, cross-sectional SEM images of the TiO_2 thin films prepared at 473 K and 873 K are displayed in Fig. 5.9. Top views of the SEM images for these thin films were almost the

same as the above AFM images. Clear differences between the UV and visible light responsive TiO_2 thin films could be observed in their cross sectional views. The film prepared at 473 K has a structure in which nano-sized TiO_2 particles randomly sintered with each other. On the other hand, the films prepared at 873 K were found to possess a unique and characteristic structure in which TiO_2 single crystals with a columnar structure (diameter: ca. 100 nm) are orderly aligned. This unique structure could be observed only when the TiO_2 thin films were prepared at relatively higher temperatures by the RF-MS method. From these investigations, the high transparency of these TiO_2 thin films were found to be associated with the construction of an assembly of closely packed TiO_2 particles with small surface roughness. On the other hand, the efficient absorption of visible light may be associated with their characteristic structures, such as the orderly aligned columnar TiO_2 crystals, obtained only by the RF-MS method. For further studies on the mechanism of the absorption of visible light, depth profiles of the O/Ti atomic ratio were investigated by AES measurements. As shown in Fig. 5.10, the O/Ti atomic ratio of the transparent TiO_2 thin film prepared at 473 K was constant at 2.0 from the surface to deep bulk, suggesting a stoichiometric TiO_2 composition. On the other hand, the O/Ti atomic ratio of the visible light-responsive TiO_2 thin film prepared at 873 K was found to decrease gradually from surface to deep bulk reaching about 1.933. Such a declined

structure in the O/Ti atomic ratio for the visible light-responsive TiO_2 thin films was confirmed to be stable even after calcination at 773 K, since the stoichiometric TiO_2 layer at the surface (thickness; ca. 100 nm) worked as a passive layer to protect the bulk sections. Moreover, the declined structure may be closely associated with the modification of the electronic properties of the TiO_2 semiconductor, enabling the efficient absorption of visible light. It has already been reported that small amounts of oxygen vacancies in the TiO_2 lattice give rise to the distortion of the TiO_2 octahedral unit and weaken the Ti-O bonds, resulting in a reduction of the splitting between the bonding and nonbonding levels [26]. However, the further investigations on the role of the oxygen vacancy for the absorption of visible light are yet necessary. Taking these results into consideration, such a characteristic declined composition of the TiO_2 thin films may be the determining factor in modifying the electronic properties so that they are able to operate as efficient photocatalysts even under visible light irradiation.

5.4. Conclusions

Transparent TiO_2 thin films which operate efficiently as a photocatalyst under UV and visible light irradiation were successfully developed using a single process by controlling

the preparation conditions such as the target material, sputtering gas and preparation temperatures in a RF-magnetron sputtering (RF-MS) deposition method. The TiO_2 thin films prepared at relatively low temperatures ($T < 473$ K) showed high transparency and effective photocatalytic reactivity for the decomposition of NO as well as the oxidation of various organic compounds under UV light irradiation. On the other hand, the thin films prepared at relatively high temperatures ($T > 773$ K) exhibited a pale yellow color, indicating that these thin films can absorb visible light efficiently so that much higher photocatalytic reactivity for the above reactions were possible even under visible light irradiation. From various characterization studies of these thin films, the unique structure of the orderly aligned columnar TiO_2 single crystals could be observed along with a declined structure in which the O/Ti atomic ratio slightly decreased from surface to deep bulk. These characteristic structural factors are considered to play an important role in the efficient modification of the electronic properties of these TiO_2 semiconductors, enabling the absorption of visible light. These findings are expected to open the way to new possibilities in the widespread and cost-efficient production of visible light-responsive TiO_2 photocatalysts that can utilize safe and clean solar energy for beneficial purposes.

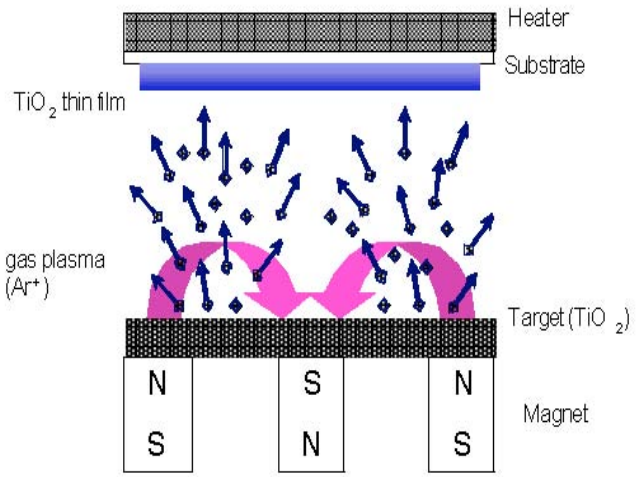

Figure 5.1 Schematic diagram of the RF magnetron sputtering (RF-MS) deposition method.

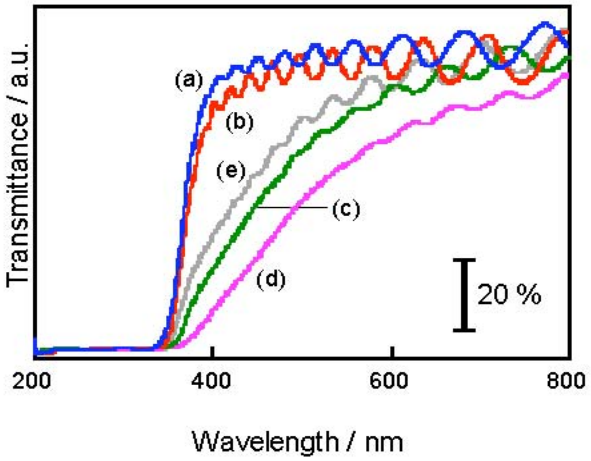

Figure 5.2 UV-Vis absorption spectra of the TiO_2 thin films prepared at: (a) 373, (b) 473, (c) 673, (d) 873 and (e) 973 K.

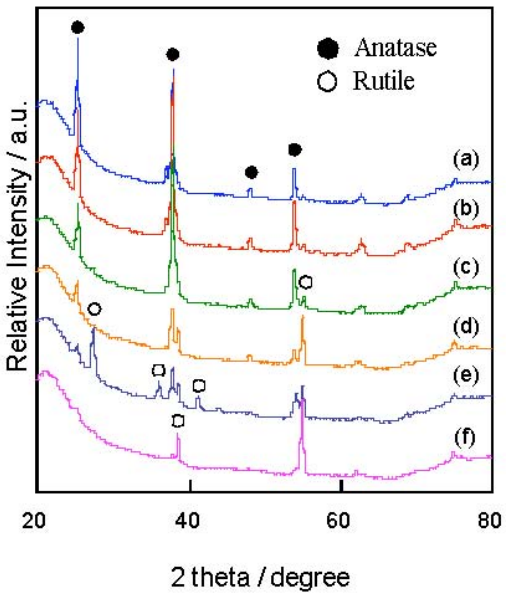

Figure 5.3 XRD patterns of the TiO_2 thin films prepared at: (a) 473, (b) 573, (c) 673, (d) 773, (e) 873 and (f) 973 K.

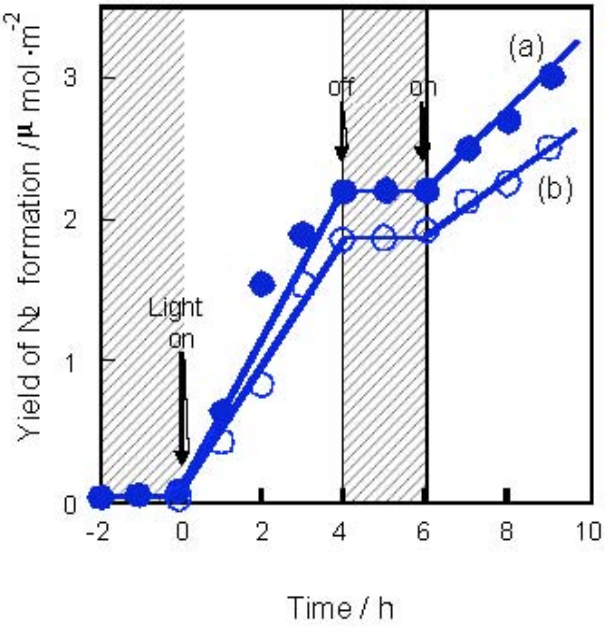

Figure 5.4 Reaction time profiles of the photocatalytic decomposition of NO on: (a) the transparent TiO_2 thin film prepared at 473 K; and (b) the commercial TiO_2 powder (Degussa, P-25) under UV light ($\lambda > 270$ nm) irradiation at 275 K.

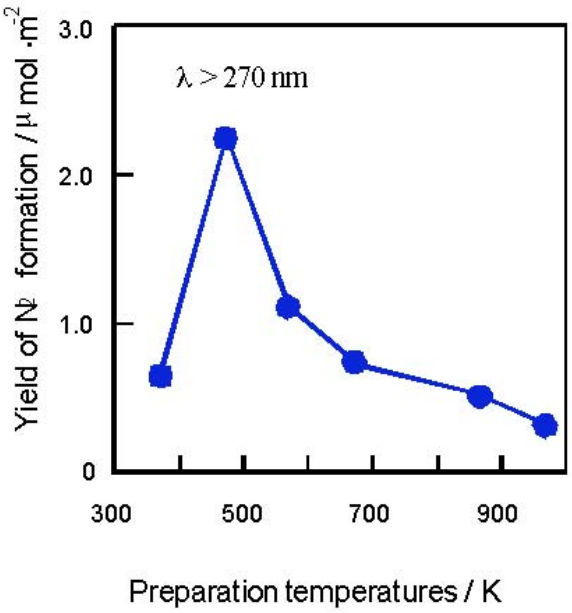

Figure 5.5 Effect of the preparation temperatures on the photocatalytic reactivity of the TiO_2 thin films for the decomposition of NO under UV light ($\lambda > 270$ nm) irradiation.

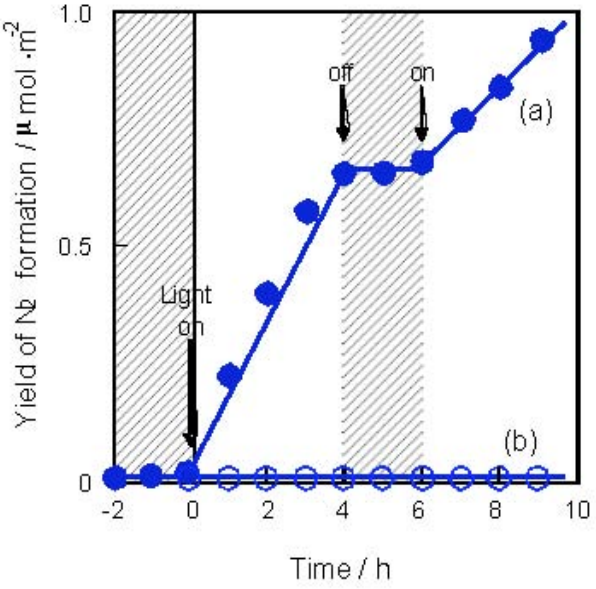

Figure 5.6 Reaction time profiles of the photocatalytic decomposition of NO on: (a) the visible light responsive TiO_2 thin film prepared at 873 K; and (b) the commercial TiO_2 powder (Degussa, P-25) under visible light (λ> 450 nm) irradiation at 275 K.

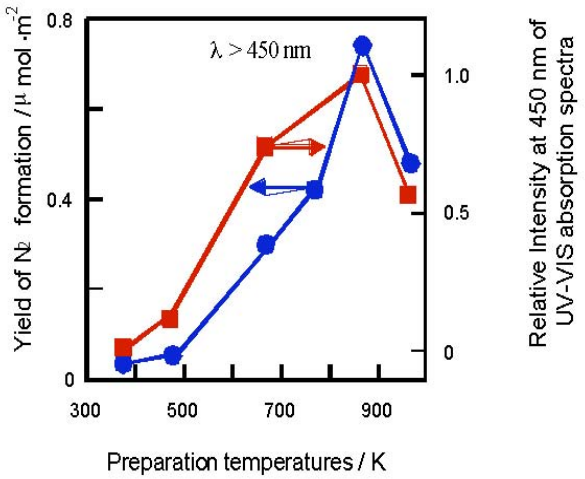

Figure 5.7 Effect of the preparation temperatures on the photocatalytic reactivity for the decomposition of NO under visible light ($\lambda > 450$ nm) irradiation as well as the relative intensities at 450 nm in the UV-Vis absorption spectra.

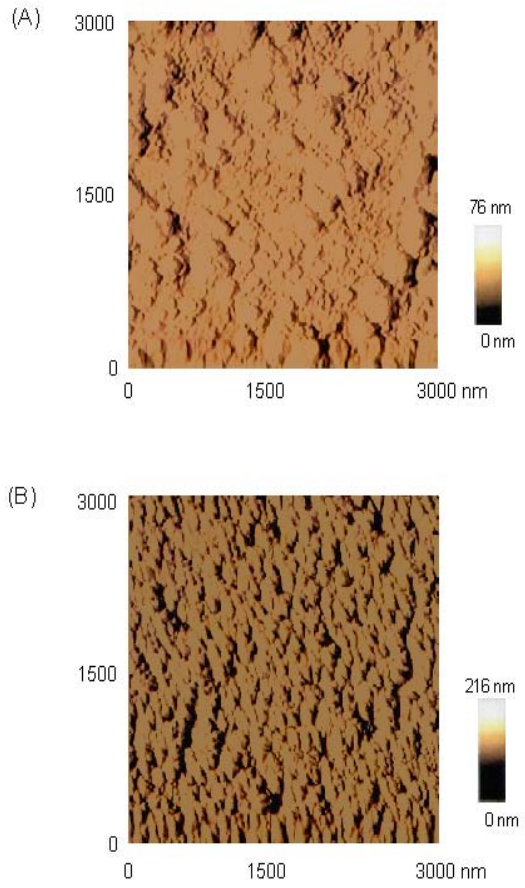

Figure 5.8 AFM images of the TiO_2 thin film prepared at (A) 473 K and (B) 873 K.

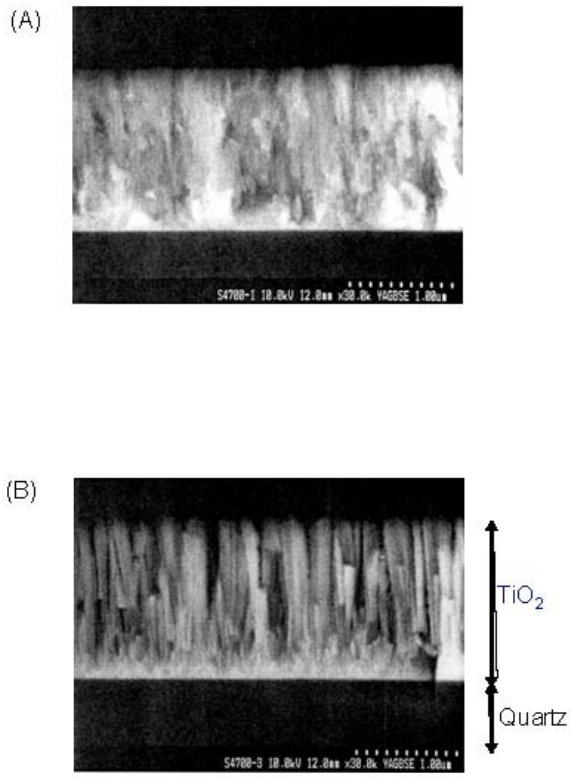

Figure 5.9 Cross-sectional SEM images of the TiO_2 thin film prepared at (A) 473 K and (B) 873 K.

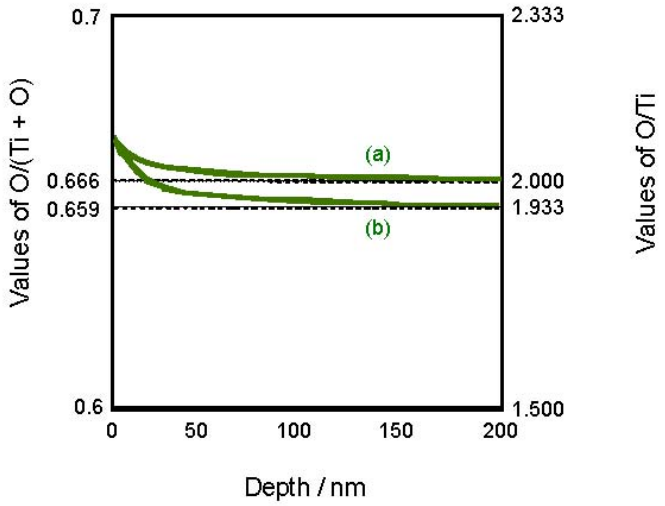

Figure 5.10 Depth profiles of the O/(Ti+O) and O/Ti ratios as determined by AES measurements for the TiO_2 thin films prepared at (a) 473 K and (b) 873 K.

Preparation temperature (K)	Particle size (nm)	Crystal phase
473	18.4	Anatase
573	16.5	Anatase
673	18.9	Anatase
773	21.4	Anatase
873	20.8	Rutile (mainly)
973	---	Rutile

Scherrer's equation: $D = K\lambda / \beta cos\theta$

D : particle size (nm)

λ : wavelength of CuKα (0.15405 nm)

β : half width (rad)

θ : Bragg angle (degree)

K : constant (in this case: 0.9)

Table 5.1. Particle sizes determined by the results of XRD measurements.

5.5. References

[1] A. Fujishima, T. N. Rao, and D. A. Tryk, J. Photochem. Photobiol. C, **1** (2000) 21.

[2] D. A. Tryk, A. Fujishima, K. Honda, Electrochimica Acta, **45** (2000) 2363.

[3] A. Fujishima, K. Hashimoto and T. Watanabe, "TiO_2 PHOTOCAATALYSIS, Fundamental and Applications" BKC, Inc., Tokyo (1999).

[4] Y. Paz, Z. Luo, L. Rabenberg, A. Heller, J. Mater. Res., **10** (1995) 2842.

[5] A. Heller, Acc. Chem. Res., **28** (1995) 503.

[6] N. Negishi, T. Iyoda, K. Hashimoto and A. Fujishima, Chem. Lett., (1995) 841.

[7] N. Negishi, K. Takeuchi and T. Ibusuki, J. Mater. Sci., **33** (1998) 1.

[8] K. L. Siefering, and G. L. Griffin, J. Electrochem. Soc., **137** (1990) 814.

[9] T. Maruyama, and S. Arai, Solar Energy Mater. & Solar Cells, **26** (1992) 323.

[10] N. Tanaka, S. Ohshio, and H. Saitoh, J. Ceram. Soc. Jpn., **105** (1997) 551.

[11] H. J. French, W. Kulisch, M. Kuhr, and R. Kassing, Thin Solid Films, **201** (1991) 327.

[12] W. G. Lee, S. I. Woo, J. C. Kim, S. H. Choi, and K. H. Oh, Thin Solid Films, **237** (1994) 105.

[13] Y. Kamishiro, Y. Kinoshita, Y. Takaoka, and S. Murasawa, J. Ceram. Soc. Jpn., **101** (1993) 514.

[14] M. Takeuchi, H. Yamashita, M. Matsuoka, T. Hirao, N. Itoh, N. Iwamoto and M. Anpo, Catal.

Lett., **66** (2000) 185.

[15] H. Yamashita, M. Anpo, Catal. Surveys Asia, 8 (2004) 1.

[16] M. Anpo, Bull. Chem. Soc. Jpn., 77 (2004) 1.

[17] M. Takeuchi, H. Yamashita, M. Matsuoka, T. Hirao, N. Itoh, N. Iwamoto and M. Anpo, Catal. Lett., **67** (2000) 135.

[18] B. Kraeutler, and A. J. Bard, J. Am. Chem. Soc., **100** (1978) 5985.

[19] A. Sclafani, L. Palmisano, M. Schiavello, V. Augugliano, S. Coluccia, and L. Marchese, New J. Chem., **12** (1988) 129.

[20] D. S. Muggli, S. A. Keyser, and J. L. Falconer, Catal. Lett., **55** (1998) 129.

[21] D. S. Muggli, J. T. McCue, and J. L. Falconer, J. Catal., **173** (1998) 470.

[22] M. Kitano, M. Tsujimaru, M. Anpo, Appl. Catal. A: Gen., **314** (2006) 179.

[23] H. Kikuchi, M. Kitano, M. Takeuchi, M. Matsuoka, M. Anpo, P.V. Kamat, J. Phys. Chem. B, **110** (2006) 5537.

[24] M. Kitano, M. Takeuchi, M. Matsuoka, J.M. Thomas, M. Anpo, Cat. Today, **120** (2007) 133.

[25] M. Matsuoka, M. Kitano, M. Takeuchi, M. Anpo, J. M. Thomas, Topics Catal., **35** (2005) 305.

[26] S. A. Bilmes, P. Mandelbaum, F. Alvarez, and N. M. Victoria, J. Phys. Chem. B, **104**

(2000) 9851.

Chapter 6

General Conclusions

6. General Conclusions

In this thesis, the study of the preparations of TiO_2 nano-particle photocatalysts by a multi-gelation method and, suppressed recombination of electrons and holes and its role in the improvement of the photoreactivity of flame-synthesized TiO_2 nanopowders, enhancement of the photocatalytic reactivity of TiO_2 nano-particles by a simple mechanical blending with hydrophobic MOR zeolites, and preparation of the visible light responsive TiO_2 thin film photocatalysts by a RF-magnetron sputtering deposition method have been investigated.

The main results obtained have been summarized below.

Summary of Chapter2

Chapter2 deals with the synthesis, characterization and photocatalytic performance of TiO_2 nanopowders prepared by a flame-synthesis method. The Anatase phase-rich TiO_2 nanopowders containing small amounts of the rutile phase were fabricated by the flame method. The photoexcited states of the TiO_2 nanopowders were directly determined by in-situ NEXAFS measurements under UV light irradiation. The present findings give direct experimental evidence by the in-situ NEXAFS showing, for the first time, that the electrons trapped in the anatase/rutile grain boundary suppress the recombination of electrons and holes, and in turn, this suppression of recombination directly contributes to an improvement in the photocatalytic reactivities for the decomposition of 2-propanol.

Summary of Chapter3

Chapter3 deals with the TiO_2 photocatalysts prepared by a multi-gelation method and the effect of the changes in the pH during the pH swing times, i.e., by a controlled pH swing, on the morphology of the TiO_2 particles. TiO_2 photocatalysts prepared by a controlled pH swing method could retain the anatase phase even at calcination temperatures of 750 °C at higher pH swing numbers. However, other important parameters such as particle size, surface area, pore volume, pore size as well as the anatase/rutile phase ratio could not be controlled well by this method. The addition of HCl acid during preparation showed detrimental effects on the morphology of the particles. On the other hand, TiO_2 catalysts prepared by an uncontrolled pH swing method showed better performance, especially in control of such important parameters. The results of 2-propanol oxidation showed that control of the anatase/rutile ratio, the pore volume as well as pore diameter of the TiO_2 nano-particles are important factors in realizing the efficient photocatalytic degradation of organic compounds.

Summary of Chapter4

Chapter4 deals with the photocatalytic oxidation of gaseous acetaldehyde with O_2 on commercial TiO_2 nano-particles. The photocatalytic properties of conventional TiO_2 nano-particles (SSP-25, Sakai Chemical Industry Co., Ltd.) could be enhanced by the simple method of mechanical blending with hydrophobic MOR zeolite powders. The optimum amount of the zeolite powders as an adsorbent for the enhancement of the photocatalytic reactivity of the blended TiO_2/MOR system was estimated to be ca. 80 - 95 wt% since the incident UV light was effectively irradiated onto the whole part of the TiO_2 nano-particles due to the high transparency of the siliceous zeolite powders. Furthermore, the hydrophobic zeolite powders efficiently gathered the gaseous acetaldehyde molecules within their cavities and supplied them onto the TiO_2 surfaces, resulting in the enhancement of the photocatalytic reactivity.

Summary of Chapter5

Chapter5 deals with the TiO_2 thin film photocatalysts which could induce photoreactions under visible light irradiation. Transparent TiO_2 thin films which operate efficiently as a photocatalyst under UV and visible light irradiation were successfully developed using a single process by controlling the preparation conditions such as the target material, sputtering gas and preparation temperatures in a RF-magnetron sputtering (RF-MS) deposition method. The TiO_2 thin films prepared at relatively low temperatures ($T < 473$ K) showed high transparency and effective photocatalytic reactivity for the decomposition of NO as well as the oxidation of various organic compounds under UV light irradiation. On the other hands, the thin films prepared at relatively high temperatures ($T > 773$ K) exhibited a pale yellow color, indicating that these thin films can absorb visible light efficiently so that much higher photocatalytic reactivity for above reactions were possible even under visible light irradiation. From various characterization studies of the visible light responsive TiO_2 thin films, the unique structure of orderly aligned columnar TiO_2 single crystals could be observed along with a declined structure in which the O/Ti atomic ratio slightly decreased from surface to deep bulk. These characteristic structural factors might play an important role in the efficient

modification of electronic properties of TiO_2 semiconductors, enabling the absorption of visible light. These findings are expected to open the way to new possibilities in the widespread and affordable production of the visible light responsive TiO_2 photocatalysts that can utilize safe and clean solar energy.

ACKNOWLEGMENTS

First of all,the author, Shirou Sakai, would like to express his sincerest gratitude to Professor Masakazu Anpo of the Department of Applied Chemistry, Graduate School of Engineering, Osaka Prefecture University, for his strong support and valuable instruction throughout this study.

Sincere thanks are also extended to Professor Hiroshi Inoue and Professor Masahiro Tatsumisago of Osaka Prefecture University for their critical reading of this thesis and many useful suggestions for its improvement.

The author would also like to thank Associate Professor Masaya Matsuoka and Research Associate Dr. Masato Takeuchi of Osaka Prefecture University for their helpful discussions and suggestions during the present research.

Finally, the author wishes to deeply thank his wife, Yuka Sakai, his parents, Meiki Sakai and Yoshiko Sakai, and his children, Yuuki, Moeko, and Maiko Sakai for their kind support and warm encouragement.

Shirou Sakai

2010, February

Sakai, Osaka

LIST OF PUBLICATIONS

1. New Trends in the Nanoscience and Nanotechnology of

Titanium Oxide-based Photocatalysts as an Environmentally-friendly Catalyst

Masato Takeuchi ,Shirou Sakai ,Afshin Ebrahimi,Masaya Matsuoka ,

Masakazu Anpo

Proc. in Nanosci. Nanotec. Conf., 5-10 (Turkey, Istanbul, 2008).

2. Surppressed Recombination of Electorons and Holes and its role the improvement of Photoreactvity of Flame-synthesizd TiO_2 Nanopowders

Hoon Park,Hyunseock Jie, Keun-Hwa Chae, Shinya Higashimoto,

Shirou Sakai, Masakazu Anpo,Jong-Ku Park, Dok-Yol Lee

submitted to *Res.Chem.Intermed.*, (2010)

3. Preparation of TiO2 nano-particle photocatalysts by a multi-gelation method: The effect of pH change

Bernaurdshow Neppolian,Diana Eddy Rakhmawaty,Shiro Sakai ,

Yoshimi Okada,Hiroaki Nishijima,Masakazu Anpo

Res.Chem.Intermed.,Vol.34,103-111(2008)

4. Enhancement of the photocatalytic reactivity of TiO_2 nano-particles by a simple mechanical blending with hydrophobic mordenite (MOR) zeolite

Masato Takeuchi , Junichi Deguchi , Manabu Hidaka , Shiro Sakai , Kyoungja Woob, Pyuck-Pa Choi , Jong-Ku Park , Masakazu Anpo

Applied Catalysis B: Environmental, 89, 406-410 (2009).

5. Preparation of Visible Light-Responsive TiO_2 Thin Film Photocatalysts by a RF-magnetron Sputtering Deposition Method

Masato Takeuchi ,Shiro Sakai , Masaya Matsuoka, Masakazu Anpo

Res.Chem.Intermed.,Vol.35,973-983(2009)

6. Application of Highly Functional Ti-oxide-based Photocatalysts in Clean Technologies

Masato Takeuchi , Shiro Sakai , Afshin Abrahimi ,Masaya Matsuoka, Masakazu Anpo

Topics in Catalysis, 52, 1651-1659 (2009).

本論文の基礎となる発表論文

No.	論文題目	著者名	発表誌名	本論文との対応
1	New Trends in the Nanoscience and Nanotechnology of Titanium Oxide-based Photocatalysts as an Environmentally-friendly Catalyst	M. Takeuchi S. Sakai A. Ebrahimi M. Matsuoka M. Anpo	Proc. Nanosci. Nanotech. Conf., pp. 5-10 (Turkey, Istanbul, 2008).	第 1 章
2	Suppressed Recombination of Electorons and Holes and its Role for the Improvement of Photoreactvity of Flame-synthesizd TiO_2 Nanopowders	H. Park H. Jie K.-H. Chae S. Higashimoto S. Sakai M. Anpo J.-K. Park D.-Y. Lee	submitted to Res. Chem. Intermed.	第 2 章
3	Preparation of TiO_2 Nano-particle Photocatalysts by a Multi-gelation Method: The Effect of pH Change	B. Neppolian D. Rakhmawaty S. Sakai Y. Okada H. Nishijima M. Anpo	Res. Chem. Intermed., Vol. 34, pp. 103-111 (2008).	第 3 章
4	Enhancement of Photocatalytic Reactivity of TiO_2 Nano-paricles by a Simple Mechanical Blending with Hydrophobic Mordenite (MOR) Zeolite	M. Takeuchi J. Deguchi M. Hidaka S. Sakai K. Woo P.-P. Choi J.-K. Park M. Anpo	Appl. Catal. B: Environmental, Vol. 89, pp. 406-410 (2009).	第 4 章
5	Preparation of Visible Light-responsive TiO_2 Thin Film Photocatalysts by a RF-magnetron Sputtering Deposition Method	M. Takeuchi S. Sakai M. Matsuoka M. Anpo	Res. Chem. Intermed., Vol. 35, pp. 973-983 (2009).	第 5 章

6	Application of Highly Functional Ti-oxide-based Photocatalysts in Clean Technologies	M. Takeuchi S. Sakai A. Ebrahimi M. Matsuoka M. Anpo	Top. Catal., Vol. 52, pp. 1651-1659 (2009).	第 5 章